



HAL
open science

Surviving glaciations in the Mediterranean region: an alternative to the long-term refugia hypothesis

Jérémy Migliore, Alex Baumel, Agathe Leriche, Marianick Juin, Frederic Medail

► To cite this version:

Jérémy Migliore, Alex Baumel, Agathe Leriche, Marianick Juin, Frederic Medail. Surviving glaciations in the Mediterranean region: an alternative to the long-term refugia hypothesis. *Botanical Journal of the Linnean Society*, 2018, 187 (4), pp.537-549. 10.1093/botlinnean/boy032 . hal-01851862

HAL Id: hal-01851862

<https://hal.science/hal-01851862>

Submitted on 31 Jul 2018

HAL is a multi-disciplinary open access archive for the deposit and dissemination of scientific research documents, whether they are published or not. The documents may come from teaching and research institutions in France or abroad, or from public or private research centers.

L'archive ouverte pluridisciplinaire **HAL**, est destinée au dépôt et à la diffusion de documents scientifiques de niveau recherche, publiés ou non, émanant des établissements d'enseignement et de recherche français ou étrangers, des laboratoires publics ou privés.

Surviving to glaciations in the Mediterranean region: an alternative to the long-term refugia hypothesis

JÉRÉMY MIGLIORE^{1,2*}, ALEX BAUMEL¹, AGATHE LERICHE¹, MARIANICK JUIN¹ and FRÉDÉRIC MÉDAIL¹

¹*Aix Marseille Univ, Avignon Université, CNRS, IRD, Institut Méditerranéen de Biodiversité et d'Ecologie marine et continentale (IMBE), Aix-en-Provence, France.*

²*Current address: Université Libre de Bruxelles, Evolutionary Biology and Ecology, Faculté des Sciences, CP160/12, 1050 Bruxelles, Belgium.*

*Corresponding author. E-mail: jeremy.migliore@imbe.fr / migliore.jeremy@libertysurf.fr

Short running head: Response of *Myrtus communis* to climate changes

Word count: 6,593 (200 abstract + 4,643 main text + 1,750/68 references)

Figure count: 4 in colours / **Table count:** 1

Supporting information: 6 figures and 2 tables

ABSTRACT

The simultaneous study of species distribution modelling (SDM) and genetic imprints left by range dynamics is appropriate when examining the biogeographical processes that have favoured the survival of plants through past climate changes. Nevertheless, such an approach is rarely performed on the scale of the entire Mediterranean and almost never concerns widespread thermophilous plants. Here, we examine the biogeographical responses of an important Mediterranean shrub, *Myrtus communis* (Myrtaceae) to severe Quaternary climate conditions. Our analysis combines SDM and phylogeography based on plastid/nuclear DNA sequences and AFLP data. Palaeoclimatic models using MAXENT and levels of genetic diversity in *M. communis* are used to infer drastic changes in areas of climatic suitability during the last 130,000 years, with a southward range contraction during the Last Glacial Maximum. Modelling of past suitability areas for myrtle identifies a few relatively small long-term refugia, suggesting that it survived in temporary refugia during glacial periods. *Myrtus communis* is characterized by a higher genetic diversity and originality in the southern part of its range, where it was less impacted by glaciations. Structure of genetic diversity reveals stronger range expansions in the Western part of the range whereas migration processes remained much more restricted in the Eastern Mediterranean.

ADDITIONAL KEYWORDS: Mediterranean –*Myrtus communis* (myrtle) – palaeoecology – phylogeography – Quaternary glaciations – range shift – refugia – species distribution modelling

INTRODUCTION

Mediterranean-climate ecosystems harbour the world's richest extra-tropical floras, but contemporary ecological factors and environmental heterogeneity do not entirely explain their remarkable biodiversity and endemism or their spatial patterns (Rundel *et al.*, 2016). It has been suggested for the Cape Region and south-western Australia that long-term environmental stability allowed ancient lineages to continue their diversification (Cowling *et al.*, 2015). By contrast, clades are generally younger in the Mediterranean region, leading to the hypothesis that environmental instability has prevented the long-term accumulation of diversity (Valente & Vargas, 2013; Cowling *et al.*, 2015). Indeed, several old lineages, *i.e.* those of early to middle Cenozoic origins, were pruned by extinction around 3.2 Ma, during the transition from a tropical to a Mediterranean climate (Postigo Mijarra *et al.*, 2009; Rodríguez-Sánchez *et al.*, 2010). The Quaternary glaciations starting at *ca.* 2.7 Ma subsequently led to an increased climatic severity characterized by more arid conditions and a mean temperature of the coldest month about 12°C cooler than at present (Wu *et al.*, 2007). These drastic climatic conditions have favoured open landscapes of grasslands and steppe vegetation to the detriment of more thermophilous and woody vegetation (Quézel & Médail, 2003; Thompson, 2005). Nevertheless, recent phylogenetic evidence suggest that most of plant clades of the Mediterranean region diversified between the Miocene and Pliocene (from 23 Ma), *i.e.* before the onset of the Mediterranean climate (Vargas, Fernández-Mazuecos, & Heleno, 2018), so that extinction of older lineages was counteracted by diversifying processes in younger lineages.

Species Distribution Models (SDM) fitted with palaeoclimatic explanatory variables can provide insights into the processes shaping modern genetic and species diversity while tracking the contraction/expansion of populations in response to successive Quaternary glacial/interglacial oscillations (Waltari *et al.*, 2007; Carnaval *et al.*, 2009). The hypothesis of long-term refugia proposes the stability of suitable areas that allow viable populations to persist through climatic oscillations (Ashcroft, 2010; Stewart *et al.*, 2010). Within the framework of refuge theory, we should expect to find a positive correlation between the stability of suitable areas and genetic singularity, since long term populations tend to harbour more diversity than recently expanding ones (Svenning *et al.*, 2011; Hampe *et al.*, 2013; Gavin *et al.*, 2014). These long-term refugia have been defined as 'phylogeographical hotspots', *i.e.* significant reservoirs of unique genetic diversity of Mediterranean plant species that probably played a key role in speciation processes (Médail & Diadema, 2009).

The complex spatio-temporal trajectories of species and populations in and out of refugia need to be better integrated (Gavin *et al.*, 2014). Combining palaeoclimatic SDM and phylogeography facilitates inferring the existence of putative Quaternary long-term refugia. This was the case for the olive tree (*Olea europaea* L.), of which a large part of its populations located in the south-western and the coastal eastern Mediterranean persisted under continuously suitable areas during the Last Inter-Glacial (LIG, *ca.* 116-130 ka BP), the Last Glacial Maximum (LGM, *ca.* 19-26.5 ka), and current climatic conditions (Besnard *et al.*, 2013).

The simultaneous analysis of both SDM and genetic imprints left by range dynamics have been rarely performed on the scale of the entire Mediterranean and even less concerning widespread thermophilous plants. In this context, we have chosen to focus on the myrtle, or *Myrtus communis* L. (Myrtaceae), because it is one of the few Mediterranean thermophilous evergreen shrubs occurring in coastal and lowland environments, below an altitude of 500 m. Indeed, a few common woody plants of the thermo-Mediterranean shrublands have been studied using a phylogeographical approach (*Pinus pinea* L.: Vendramin *et al.*, 2008; *Cistus monspeliensis* L.: Fernández-Mazuecos & Vargas, 2010; *Chamaerops humilis* L.: García-Castaño *et al.*, 2014;

Guzmán *et al.*, 2017). The myrtle is characterized by a long biogeographical history, having persisted in the Mediterranean region through the Cenozoic since at least the Neogene period (Migliore *et al.*, 2012). Found primarily in low-altitude habitats, this shrub has probably been highly impacted both by climatic and habitat changes through latitudinal shifts of climatic conditions and eustatic oscillations of the Mediterranean sea (Pirazzoli, 2005). Thus, the framework of the expansion/contraction model (Bennett & Provan, 2008; Gavin *et al.*, 2014) could be relevant for past *Myrtus* range dynamics, especially during the Quaternary climatic oscillations.

To examine the biogeographical responses of this Mediterranean shrub to severe Quaternary climate conditions, we used MAXENT species distribution models, and detected the current and past suitable areas for *M. communis* on the scale of its entire Mediterranean and Macaronesian distribution range. From this we inferred potential range shifts and identified refugia on the basis of bioclimatic suitability during the Last Inter-Glacial, the Last Glacial Maximum, and the Mid-Holocene (*ca.* 6 ka BP). We compared the implications of the SDM study with the phylogeography of *M. communis* based on plastid and nuclear DNA sequences as well as multilocus AFLP (Amplified Fragment Length Polymorphism) markers.

MATERIAL AND METHODS

MODELLING OF SUITABLE AREAS FOR *MYRTUS COMMUNIS*

Occurrence data

The study area was divided into a grid of 3,019 1 km × 1 km cells using ARCGIS 10.2 (ESRI, Redlands, USA). All the cells under consideration were at least 75% emerged land area. An occurrence dataset, consisting of 4,168 observations of *M. communis*, was (Figure 1A), collected from the following sources: the Global Biodiversity Information Facility data portal (2,011 occurrences; <http://www.gbif.org/>), and our own field GPS data (179 Mediterranean occurrences), GPS data from the French CBNMED database (758 occurrences; <http://flore.silene.eu>), the Atlas of the Aegean Flora (462 occurrences; A. Strid, unpubl. data), Flora Croatica (660 occurrences; Nikolić, 2015), and scientific literature on the flora of northern Africa and Italy (98 occurrences). For modelling purposes, the dataset was reduced to one occurrence per unit cell ($n = 3019$).

Bioclimatic variables

Six variables related to the ecological requirements of the species were chosen and used to fit the bioclimatic distribution model of *M. communis*. Isothermality (BIO3) reflects the influence of larger or smaller temperature fluctuations within a month, relative to the year (generally useful for insular and maritime environments). Minimal temperature of the coldest month (BIO6) quantifies potentially lethal frost events and generalized stress due to low temperatures. Annual temperature range (BIO7) is useful for examining the effect of the ranges of annual temperature extremes. Annual precipitation (BIO12) approximates average water availability, and precipitation of the driest month (BIO14) describes the extremes associated with potentially lethal drought events and quantifies stress due to low water availability. Finally, because *M. communis* requires warmer temperatures during the wettest period of year for its germination, mean temperature in the wettest quarter (BIO8) was also considered. These bioclimatic variables were extracted from the Bioclim dataset, provided by WORLDCLIM 1.4 in a GIS-based raster format (1 x 1 km resolution; Hijmans *et al.*, 2005; O'Donnell & Ignizio, 2012). As a safeguard against redundancy among our variables, we checked that all pairwise Pearson correlation coefficients between any two of the six selected variables were below 0.71.

Modelling method

Maximum Entropy algorithm as implemented in MAXENT 3.3.1 was used to define suitable areas for *M. communis* (Phillips, Anderson, & Schapire, 2006; Phillips & Dudík, 2008). MAXENT estimates

species' suitable areas by finding the distribution of maximum entropy (*i.e.* closest to uniform) subject to the constraint that the expected value of each environmental variable (or its transform and/or interactions) under the estimated distribution matches its empirical average. The method has been shown to be well adapted to presence-only data and has consistently demonstrated performance that is competitive with other methods (Elith *et al.*, 2006; but see Yackulic *et al.*, 2013; Phillips *et al.*, 2017). Several models were fitted by investigating all feature types (linear, quadratic, and product) and all combinations of features, except for the threshold feature, which is known to fit overly conservative models. Ten replicates were performed for each model (cross-validation method). The machine learning fitting process was set to end when training gain fell below the threshold value of 0.0001, or after 3,000 iterations. The user-defined number of background points was set to 50,000, and individual points were chosen to correct for latitudinal and sampling biases (*i.e.* an oriented random selection of 50,000 points across the entire study area, paying attention to cell area, which is a function of latitude, and to sampling bias). The extrapolate function was set to 'no'.

Model selection

The Akaike Information Criterion (AIC) was calculated for all models and averaged by combination to define the most parsimonious combination of features. Area Under the Curve (AUC) and standard deviation metrics were checked for congruence with AIC results. The final model of the current suitable areas for *M. communis* was fitted using the selected combination of features, with 50 replicates (identical parameters to the fitting procedure). A Jackknife analysis was performed to evaluate variable contributions to the model, and response curves were created to assess how each variable influences the level of suitability.

Model projections and persistence assessment

The final model was projected using prior climate history to determine the suitable areas for *M. communis* during the Mid-Holocene, LGM and LIG periods. It was assumed that the ecological requirements of *M. communis* have remained similar over the last Pleistocene climatic cycles (Valiente-Banuet *et al.*, 2006; Nogués-Bravo, 2009). Reconstructed bioclimatic variables were provided by: the recently updated Coupled Model Intercomparison Project Phase 5 (WORLDCLIM 1.4); testing data from Global Climate Models (GCM) CCSM4 (Community Climate System Model); MIROC-ESM (Model for Interdisciplinary Research on Climate); and the MPI-ESM-P (Max Planck Institute Earth system model) for the Mid-Holocene (30 second resolution, *i.e.* approximately 1 × 1 km) and LGM periods (2.5 min resolution, *i.e.* approximately 5 × 5 km; this layer was resampled to a 1 × 1 km resolution raster but not interpolated, meaning the resolution of interpretation for the LGM projected model and derived inferences must be 5 × 5 km). For the LIG chronozone, data from Otto-Bliesner *et al.* (2006) were used (30 second resolution).

Suitability values as modelled by MAXENT were converted into presence/absence, using the ten-percentile threshold of 0.305571, the minimum probability for presence cells after discarding the lowest 10% of the suitability distribution (Pearson *et al.*, 2007). Long-term persistence areas were inferred as continuously suitable areas (> ten-percentile value) over the LIG, LGM and Mid-Holocene periods.

PHYLOGEOGRAPHICAL RECONSTRUCTION OF *MYRTUS COMMUNIS*

Genetic sampling strategy and molecular methods

We collected 118 samples from the entire Mediterranean and Macaronesian distribution area of *M. communis*. One randomly-sampled individual per site was newly genotyped using AFLP (Table S1; Vos *et al.*, 1995). The AFLP reaction was performed on 300 to 500 ng of DNA extract, as described in Migliore *et al.* (2011). After screening selective primers, three primer combinations

giving clearly visible band profiles were chosen (*EcoRI*-AAGG/*MseI*-CCAG, *EcoRI*-AAC/*MseI*-CAC, *EcoRI*-AAC/*MseI*-CAA). Polyacrylamide electrophoreses (0.4%) were performed using a 96-capillary automated sequencer (Megabace 1000, Amersham Bioscience), with manual scoring used to detect error-prone markers that had no reliable peak. The reproducibility of the AFLP markers was checked by repeating the complete analysis on 20 samples for each pair of primers (Bonin *et al.*, 2004). A genotyping error rate of 5.7% was obtained, due to the unreliability of some markers, which were subsequently removed from the dataset.

We also included sequence data for the plastid DNA *trnL-trnF* and *rpl2-trnH* intergenic regions, the nuclear DNA external transcribed spacer (ETS) region, and the internal transcribed spacer (ITS1-5.8S-ITS2) region, ($n = 309$ and 176 , respectively; Table S1). The methods used to extract DNA and to sequence DNA markers are described in Migliore *et al.* (2012), since these sequences were previously generated for phylogenetic reconstruction and molecular dating.

Genetic analyses

AFLP genotypes were assigned to genetically homogeneous clusters via the model-based clustering algorithm provided by STRUCTURE 2.3.3 (Pritchard, Stephens, & Donnelly, 2000; Falush, Stephens, & Pritchard, 2007). Bayesian analysis was run for 1,000,000 generations (burn-in of 100,000), and for K between 2 and 21 with ten iterations for each K -value. The admixture and recessive allele models were then chosen. The most likely number of clusters was determined using the criteria $\ln Pr(X/K)$ and ΔK (Evanno, Regnaut, & Goudet, 2005).

After independently concatenating the two plastid and the two nuclear regions, plastid haplotype and nuclear ribotype median-joining networks were constructed, using NETWORK 4.613 (Bandelt, Forster, & Röhl, 1999).

To check the congruence of the genetic patterns from the same samples studied with AFLP and DNA sequences, a Mantel test was undertaken, comparing inter AFLP genotype distances (Jaccard index) to nucleotidic divergence of plastid DNA haplotypes and nuclear DNA ribotypes (p distance). The Mantel test was based on 10,000 permutations (GENALEX 6.5; Peakall & Smouse, 2012).

Genetic diversity and singularity were summarized by several indices calculated using GENALEX 6.5: the number of plastid DNA haplotypes (NH) and nuclear DNA ribotypes (NR) including private haplotypes and ribotypes; the unbiased diversity (uh) for all the markers; the mean genetic distance within each group of samples sequenced (GD); the number of AFLP bands (NB); the number of private AFLP bands (PB); and the percentage of AFLP polymorphic loci ($\%P$). All these indices were computed according to (i) the main AFLP genetic clusters detected, and (ii) the main geographical trends of climatic suitability found according to SDMs, excluding the Macaronesian genetic cluster whose sampling was too low.

RESULTS

MODELLED CURRENT AND PAST SUITABLE AREAS FOR *MYRTUS COMMUNIS*

The most parsimonious fitted model (based on AIC, Table S2, Figure 1B) was a combination of linear and quadratic features, with a True Skill Statistics (TSS) value of 0.73 (calculated using the 10-percentile threshold for a binary transformation; and an AUC value for training data of 0.88 ± 0.0068 (gain threshold reached after 1,040 iterations). Jackknife and response curves indicated that higher suitability values were inferred with high values of “minimal temperature of coldest month” with an optimum at 6°C (*BIO6*; test gain when used in isolation (Tg) of 0.88). Suitability also increased with moderate values of “mean temperature in the wettest quarter” with an optimum at 18°C (*BIO8*; $Tg = 0.49$) and low values of “annual temperature range” (optimum = 8°C

for *BIO7*; $Tg = 0.31$). Annual precipitation values also positively influenced the suitability level ($Tg = 0.25$), with an inferred maximum suitability of 825 mm of annual precipitation. The variables “precipitation in the driest month” (*BIO14*) and “isothermality” (*BIO3*) slightly influenced the current model ($Tg = 0.025$ and 0.023 respectively). In summary, *M. communis* appeared to be particularly sensitive to cold stress, with suitable areas characterized by mean minimal temperature above frost threshold and mild winter temperatures. Areas with low level of precipitation (from 220 mm) are suitable for *M. communis*, but its optimum is around the maximum average annual precipitation value that defines the Mediterranean climate.

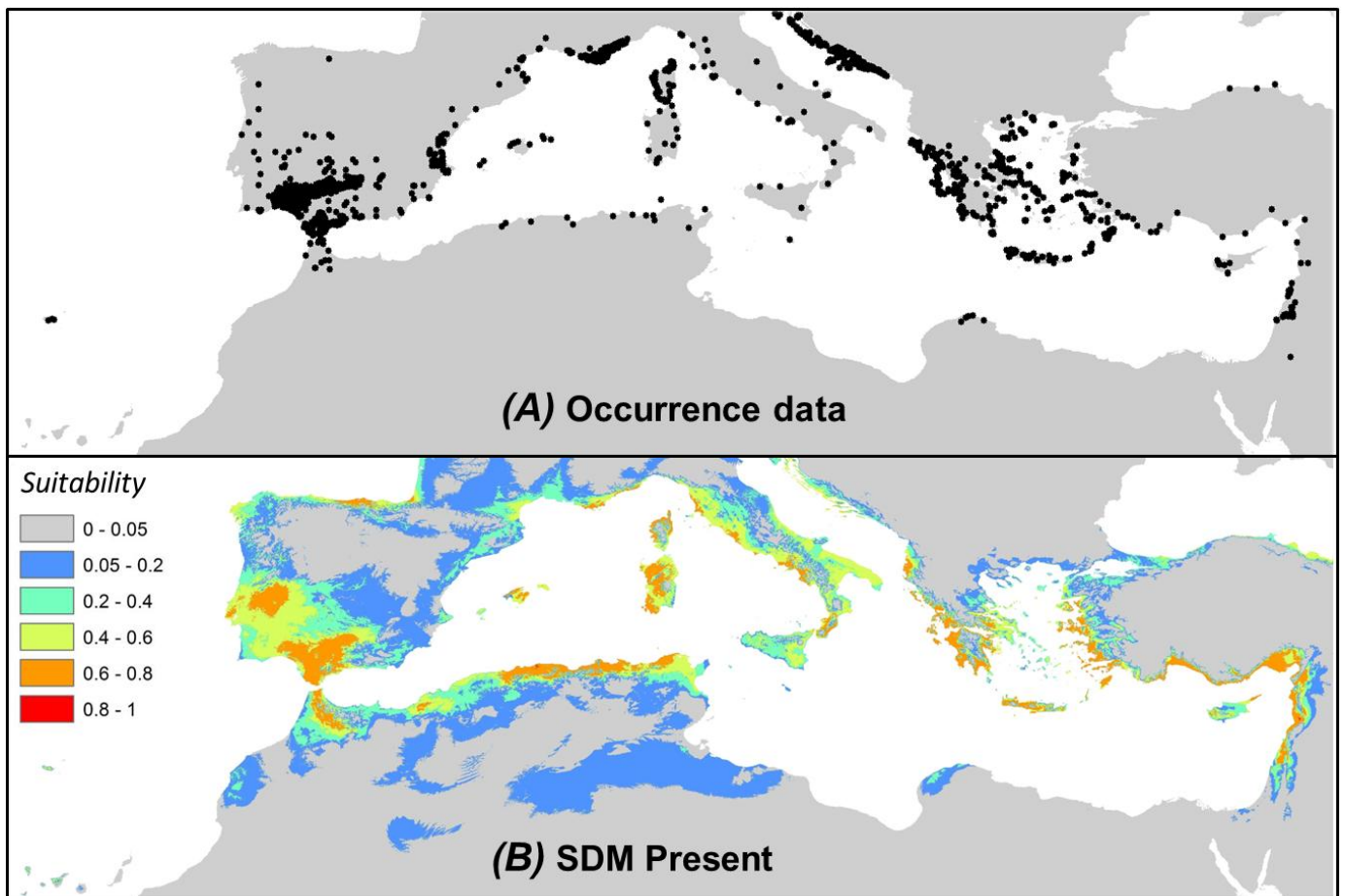


Figure 1. Known occurrences of *Myrtus communis* in the Mediterranean Basin, gathered from botanical databases and literature in addition to field collected data ($n = 4,168$) (A). Current suitable areas for the species, applying species model distribution (SDM) from actual occurrences using MAXENT with six bioclimatic variables (see Methods) (B).

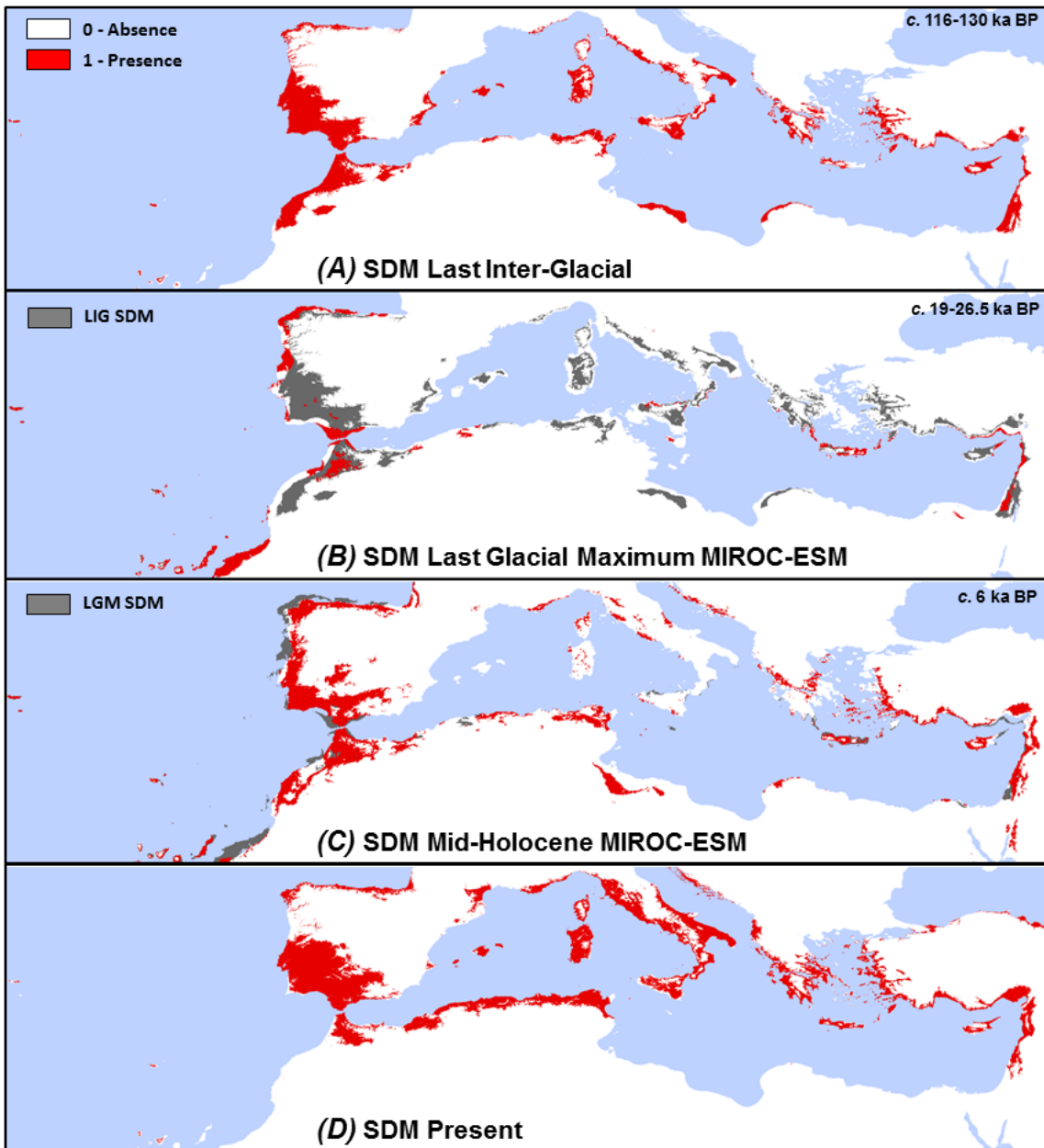


Figure 2. Suitable areas for *Myrtus communis* (projection of the most parsimonious MaxEnt model fitted to current climatic conditions from actual occurrences) during the Last Inter-Glacial (LIG) period (A), the Last Glacial Maximum (LGM) using the MIROC-ESM climate model (B), the Mid-Holocene using the MIROC-ESM climate model (C), and the Present (D). Continuous suitability values modelled with MAXENT were converted into presence/absence, using the ten-percentile threshold ≥ 0.3 (see Methods and Figures S1-4). Shading refers to palaeodistributions modelled just before the chronozone represented.

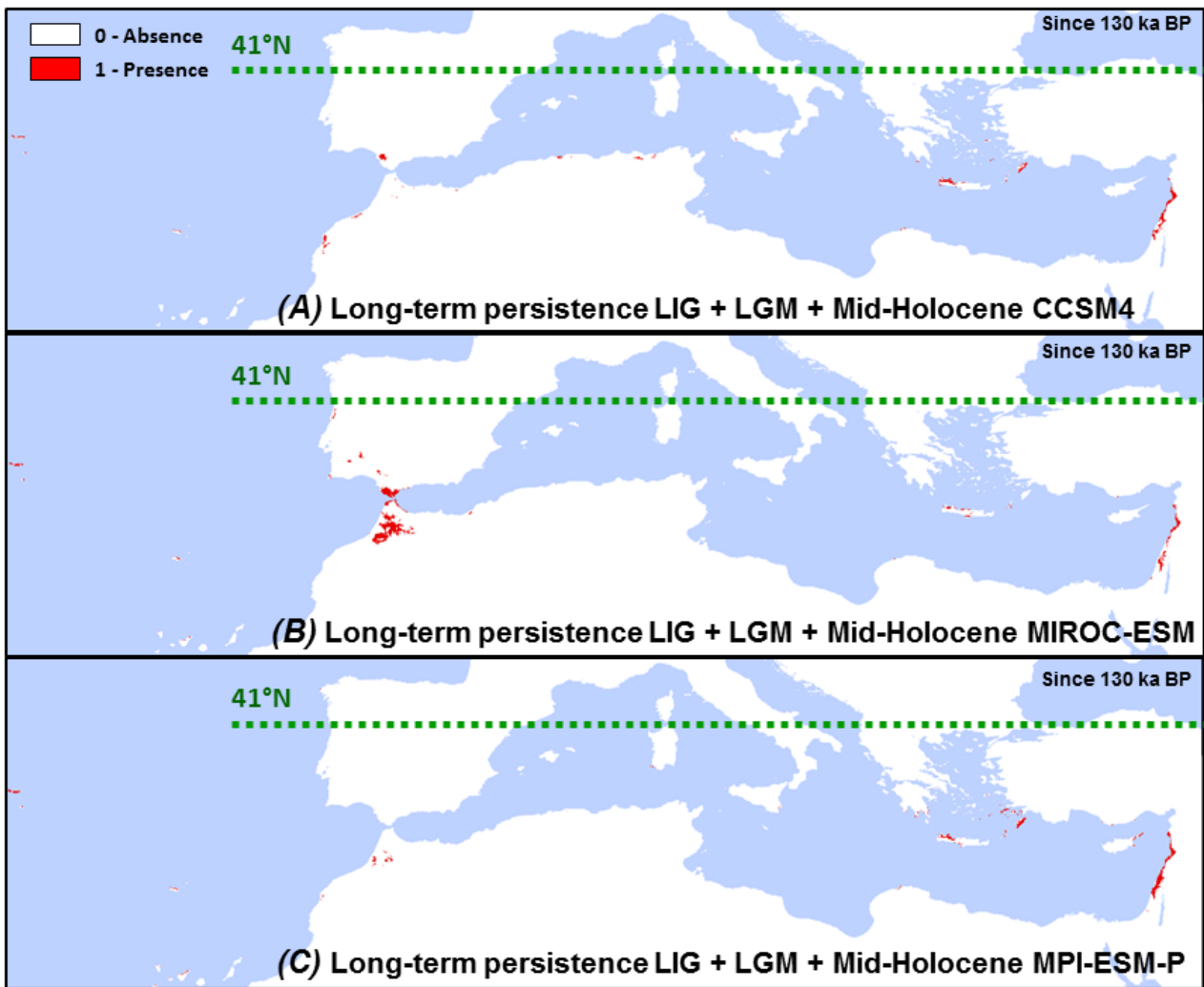


Figure 3. Long-term persistence areas inferred as continuously suitable areas over the Last Inter-Glacial (LIG) period, the Last Glacial Maximum (LGM) and Mid-Holocene using the CCSM4 (A), MIROC-ESM (B) and MPI-ESM-P (C) climate models (ten-percentile threshold ≥ 0.3 ; 5×5 km resolution).

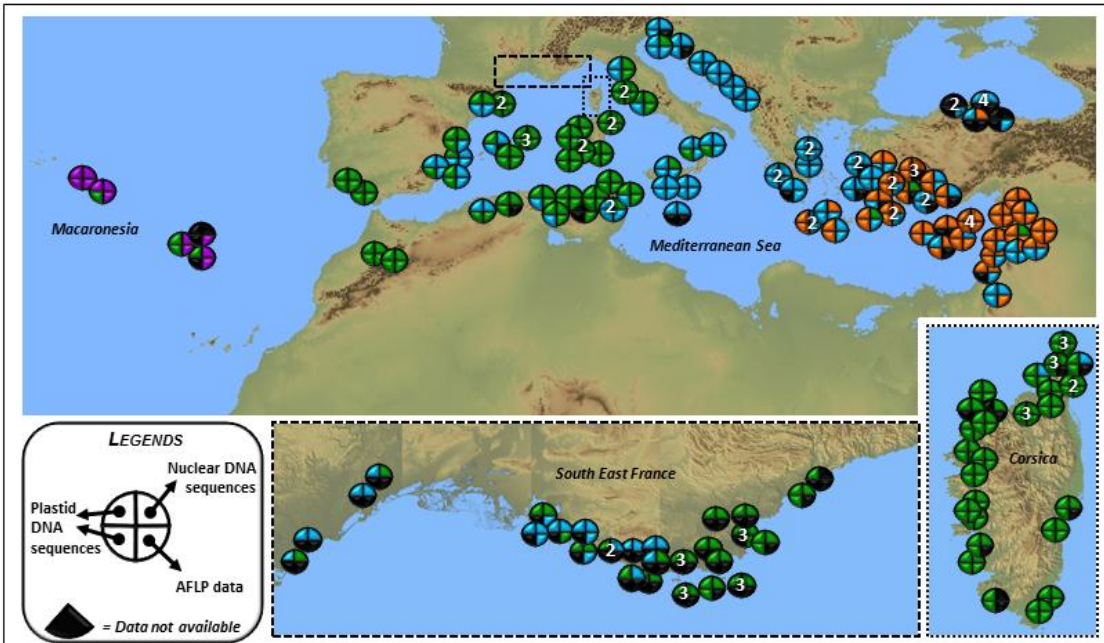
The low number of available Myrtle fossils from the LGM and Mid-Holocene periods (Migliore *et al.*, 2012) makes it difficult to choose between one of the three past climate models (CCSM4, MIROC-ESM, and MPI-ESM-P) for projecting SDM. The myrtle range dynamics over time using the MIROC-ESM climate model is the only one presented in this manuscript (Figure 2; results with the two other past climate models are presented as Supplementary Information). However, the SDM inference of long-term persistence areas is presented using all three past-climate model projections (Figure 3).

During the LIG period, *M. communis* was inferred to be potentially widespread throughout the entire Mediterranean Basin, albeit with a suitable area along the European and northern African coasts that was narrower than the current one (Figure 2A). The total inferred size of suitable areas approached 4,468,025 km² during the LIG versus 13,482,343 km² at present. A high level of suitability was suggested along the Atlantic coast (Portugal, Gibraltar, the south-western Iberian Peninsula, and western Morocco). In the eastern Mediterranean, the spatial range was similar to the current one, with a slight southward shift of suitable areas.

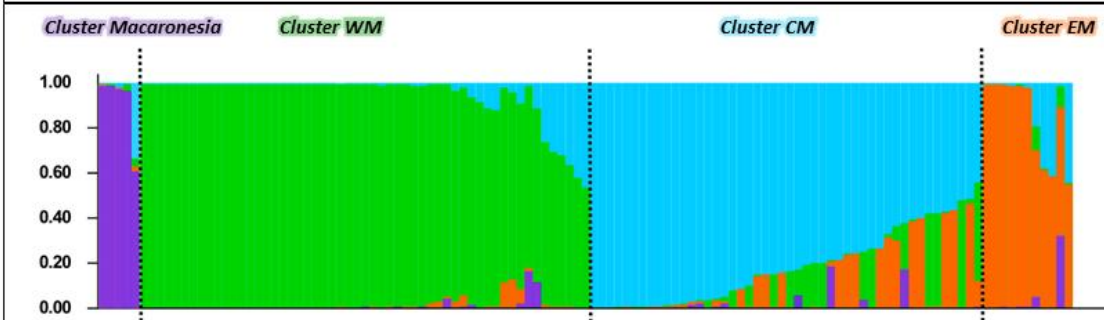
During the LGM, the whole study area was much less suitable for *M. communis* than it is under current climate conditions (Figure 2B). A drastic restriction of its potential suitable range is suggested: on average, the climate models showed 4,343,671 km² of suitable areas lost between the LIG and the LGM (Figures S1-2). We have to point out that the physiography of the Mediterranean Basin was quite different during these periods from how it is at present: in particular, the Adriatic Gulf had seen a sea-level drop of 100-120 m relative to the present. Using the LIG map as a baseline for analysing the changes occurring during the LGM, we can infer that the suitable areas for *M. communis* could have moved down towards lower altitudes and southward towards lower latitudes. This was apparent on western and central Mediterranean islands, along the Atlantic coastline, and, to a lesser degree, in Greek and Turkish areas (Figure 2B). Among the climate models used for the LGM, the CCSM4 model was the most restrictive with only 91,052 km² of suitable area, in contrast to 120,428 km² for the MIROC-ESM (with higher suitability in Iberian Peninsula and the Gibraltar Strait), and 161,585 km² for the MPI-ESM-P models (with higher suitability in western Mediterranean islands) (Figures S1-2).

During the Mid-Holocene, the climatic conditions were inferred to be more suitable than during the LGM, thus allowing for a *M. communis* range expansion (Figures 2C, S3, S4). Averaging over the three climate models, this gain in area comes to 196,412 km² in total.

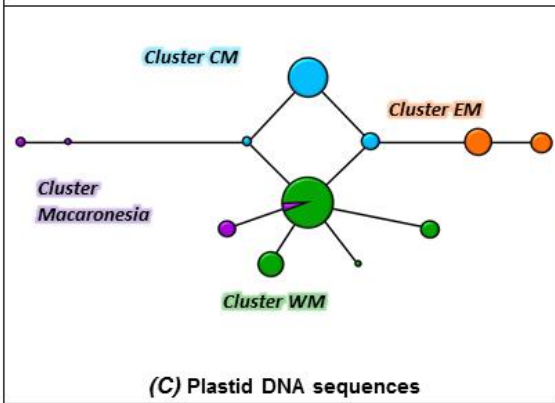
An important but unexpected result was the low number and small size of inferred long-term refugia (*i.e.* continuously suitable areas over the LIG, LGM and Mid-Holocene), whatever past-climate model is used (Figure 3). We infer drastic changes in the spatial range of the species between these periods together with a quasi-absence of overlap between suitable areas during the three contrasted climatic periods, apart from parts of the Macaronesian islands (Azores and Madeira), around the Gibraltar Strait, on the island of Crete, and in the Levant (Figure 3). Above the 41°N parallel, no long-term persistence areas over the LIG, LGM and Mid-Holocene were detected in the northern part of the Mediterranean Basin (Figure 3).



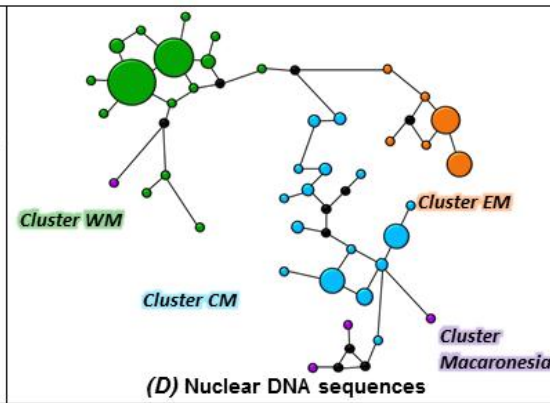
(A) Spatial genetic structure for *Myrtus communis*



(B) AFLP data



(C) Plastid DNA sequences



(D) Nuclear DNA sequences

Figure 4. Spatial genetic structure of *Myrtus communis* through its Mediterranean distribution range (A), based on the AFLP (Amplified Fragment Length Polymorphism) data summarized from STRUCTURE, based on $K = 4$ genetic clusters (B), and the median-joining networks from concatenated plastid DNA sequences *trnL-trnF* and *rp12-trnH* intergenic regions (C) and concatenated nuclear DNA sequences external transcribed spacer (ETS) region and internal transcribed spacer (ITS1-5.8S-ITS2) (D). Colour chart is based on the four main genetic clusters identified by AFLP: EM (Eastern Mediterranean in orange), WM (Western Mediterranean in green), and CM (circum-Mediterranean in blue), and Macaronesia (in purple). Numbers in the panel (A) referred to spatially-closed populations whose samples have the same genetic clusters identified. Haplotype and ribotype identifiers are detailed in Figure S6; circle sizes in networks are proportional to haplotype/ribotype frequencies.

MULTI-MARKERS GENETIC DIVERSITY OF *MYRTUS COMMUNIS*

The AFLP analysis on 118 individuals of *M. communis* resulted in 199 scored fragments, 191 of which were found to be polymorphic, with a length varying from 66 to 460 bp (dataset available on request). The most probable partitioning of the genetic variation of *M. communis* according to STRUCTURE was in $K = 2$ and $K = 4$ genetic clusters (Figures 4A-B, S5).

The genetic distances calculated from AFLP, plastid and nuclear DNA sets of data were positively correlated and the Mantel tests were significant for the Mediterranean samples ($n = 110$: plastid DNA vs AFLP: $R^2 = 0.20$, $P = 0.0001$; plastid DNA vs nuclear DNA: $R^2 = 0.19$, $P = 0.0001$; nuclear DNA vs AFLP: $R^2 = 0.20$, $P = 0.0001$). Genetic diversity indices were computed for each AFLP genetic cluster: for the three molecular markers, the Western Mediterranean (WM) and Eastern Mediterranean (EM) clusters had similar levels of diversity when accounting for the different levels of sampling (*uh*; Table 1). The circum-Mediterranean (CM) cluster had the lowest diversity of plastid DNA markers but had the highest diversity of nuclear DNA, and it also had the highest percentage of polymorphic markers for AFLP ($\%P$; Table 1). This contrast could be due to the intermediate geographical position of the CM cluster providing a higher admixture of the WM or EM clusters, *i.e.* contact zones (see below).

The plastid DNA network was characterized by 12 haplotypes (Figures 4A-C, S6A-C) geographically structured within the Mediterranean Basin and between the Macaronesian and Mediterranean regions. The simultaneous analysis of ETS and ITS nuclear DNA data revealed a similar genetic pattern to that obtained with plastid DNA data; 41 ribotypes were distributed through the three main genetic clusters (Figure 4A-D and Figure S6B-D).

Higher values of genetic singularity and diversity were detected south of the 41°N parallel (Figure 3), as follows: 9 plastid DNA haplotypes (vs 4 to the north) of which 5 (vs 0) are private; 26 ribotypes (vs 19) of which 17 (vs 11) are private; 175 AFLP bands (vs 135) of which 50 (vs 10) are private (Table 1). Higher genetic diversity in the southern Mediterranean was detected similarly for plastid DNA, nuclear DNA and AFLP molecular markers (see *uh* and $\%P$ in Table 1). Southern France and Corsica, which were the most-sampled areas in the northern Mediterranean, appeared to have a low genetic originality (no private markers) even though France was a contact zone between the WM and CM genetic clusters (Figures 4 and S6). Considering each of these clusters independently, we found that the areas harbouring the highest number of plastid DNA haplotype were situated in North Africa (WM, Algeria and Tunisia), in Sicily (CM), and in the Levant and Cyprus (EM). The number of ribotypes was also higher in North Africa (WM), the Levant, and Cyprus (EM) (Figure S6).

At the scale of the Mediterranean Basin, the contact zones between genetic clusters occurred longitudinally, and originated from WM and CM clusters, whereas plastid haplotypes and

ribotypes of the EM cluster remained isolated (Figure 4). The major plastid DNA contact zone was detected between EM and CM clusters in Turkey and the Levant, implying widespread haplotypes 4 and 12 (Figure S6). The same pattern was observed for nuclear DNA markers (AFLP and sequences), except that the WM cluster was detected in Turkey and the Levant. In summary, the three molecular markers are consistent in indicating that the Western and Central parts of the Mediterranean could have been stronger sources of range expansions than the Eastern parts.

Table 1. Genetic (plastid DNA sequences, nuclear DNA sequences and AFLP data) features for Mediterranean samples of *Myrtus communis* in relation with the three detected genetic clusters (Eastern, Circum and Western Mediterranean) and with the distribution of samples in the North or in the South of the 41°N parallel: sample size (*n*), number of plastid DNA haplotypes (*NH* with number of private haplotypes in brackets), unbiased diversity (*uh* with standard errors in brackets), mean genetic distance (*GD*), number of nuclear DNA ribotypes (*NR* with number of private nrDNA ribotypes in brackets), number of AFLP bands (*NB*), number of private AFLP bands (*PB*), percentage of polymorphic loci (*%P*).

	Plastid DNA sequences				Nuclear DNA sequences				AFLP data				
	<i>n</i>	<i>NH</i>	<i>uh</i>	<i>GD</i>	<i>n</i>	<i>NR</i>	<i>uh</i>	<i>GD</i>	<i>n</i>	<i>NB</i>	<i>PB</i>	<i>uh</i>	<i>%P</i>
Cluster EM <i>Eastern Mediterranean</i>	60	2	0.051 (0.051)	0.463	26	6	0.042 (0.021)	6.108	10	110	12	0.145 (0.013)	43.72
Cluster CM <i>Circum Mediterranean</i>	86	3	0.037 (0.028)	0.333	52	16	0.091 (0.030)	7.177	48	151	23	0.124 (0.011)	67.34
Cluster WM <i>Western Mediterranean</i>	155	4	0.055 (0.032)	0.491	94	15	0.041 (0.018)	3.831	55	132	19	0.130 (0.013)	54.27
All data	301	9	0.212 (0.057)	/	172	37	0.294 (0.035)	/	113	199	/	0.278 (0.018)	/
NM Northern Mediterranean (41°N)	133	4 (0)	0.085 (0.048)	0.768	86	19 (11)	0.186 (0.032)	8.332	43	135	10	0.161 (0.014)	56.78
SM Southern Mediterranean (41°N)	168	9 (5)	0.267 (0.061)	2.407	86	26 (17)	0.340 (0.036)	11.844	70	175	50	0.173 (0.013)	82.41

DISCUSSION

Palaeoclimatic SDM and levels of genetic diversity suggest drastic changes in suitable areas for *M. communis* during the last 130,000 years. In contrast to the phylogeography of *Olea europaea* (Besnard *et al.*, 2013), past suitability modelling hindcasts the persistence of myrtle populations in a few small long-term refugia.

Projected past suitable areas for *M. communis* indicated a strong signature of the last glaciation on the potential geographical range of the species. On average 97% of suitable areas were inferred to be lost between the LIG and the LGM (Figure 2). The decrease in genetic diversity and singularity revealed by molecular markers (Table 1) is consistent with the idea that northern populations along the Mediterranean coastline were the most affected by LGM climate change, as also evidenced by *Laurus nobilis* (Rodríguez-Sánchez & Arroyo, 2008), *Erica scoparia* (Désamoré *et al.*, 2012), and *Chamaerops humilis* (García-Castaño *et al.*, 2014). Furthermore, dramatic consequences of glaciations with major bottlenecks, or even complete extinction in the Mediterranean, were suggested for some thermophilous plants, as *Nerium oleander* L. (Mateu-Andrés *et al.*, 2015), and *Ceratonia siliqua* L. (Ramón-Laca & Mabberley, 2004).

The strong range contraction inferred for *M. communis* during the LGM raises the issue of its long-term survival through the Pleistocene. Since fossil data are often too scarce for formally validating SDM, the identification of refugia using SDM approaches remains tentative (Ashcroft, 2010). According to SDM, the size of the myrtle's long-term refugia is highly variable with (i) two main poles of persistence in the western Mediterranean (Atlantic coast and Baetic-Rifan complex) and in the east (Levantine coast), and (ii) small pockets along the mainland and island coastlines (Figure 3). The reduced overlap of suitable areas among the three palaeomaps (LIG, LGM, and Mid-Holocene) leads to a few very reduced long-term refugia compared to the size of the glacial refugia (Figures 2-3). These results, rarely found in the literature, question the long-term refugia hypothesis and suggest the possibility of a regional persistence of *M. communis* by range shifts toward temporary refugia, where conditions became suitable. It must be noted that the projections of SDM at the LIG, LGM and Mid-Holocene periods do not aim to infer *M. communis* distribution at those times, but rather to identify potential suitable areas considering the environmental variables selected. Distribution and suitable areas would be consistent only under the assumption of unlimited dispersal of the species.

At this juncture, we may examine our capacity to reject the possibility of long-term and *in situ* refugia for *M. communis* that could be cryptic for our methods. The role of local microrefugia may have played a more important role than expected, as the heterogeneity of micro-habitats may have allowed species to cope with environmental stress at finer spatial scales (Stewart & Lister, 2001; Serra-Diaz *et al.*, 2015; Meineri & Hylander, 2017). However, it is worth considering the studies conducted on *M. communis* at small scales. Studies in southern Spain are consistent with a low likelihood of long-term persistence of *M. communis* within small remnant patches of woodlands (González-Varo *et al.*, 2015). The regeneration and genetic diversity of *M. communis* are generally lower in small populations, and have a high sensitivity to fragmentation (*e.g.* González-Varo, Arroyo, & Aparicio, 2009; Nora, Albaladejo, & Aparicio, 2015). Though places such as Corsica can harbour conditions for local microrefugia (Médail & Diadema, 2009; Gavin *et al.*, 2014), local persistence is unlikely, perhaps due to the severe effects of glaciations (Conchon, 1986). Despite its abundance in the lowlands of Corsica up to 500 m of altitude, and irrespective of

which molecular marker was used, we found a lack of genetic differentiation, with for example only two plastid DNA haplotypes (8, 9) detected after an extensive sampling. These haplotypes are not private to Corsica and belong to the WM genetic cluster, occurring in Sardinia, South-east France, Italy and Eastern Algeria (Figures 4 and S6). Moreover, all the 12 Corsican palaeoecological records for *Myrtus* correspond to the late Holocene (Reille, 1977, 1984, 1992; Vella, 2010). Reille (1992) suggested that *M. communis* is “the latest arrival in the thermophilous vegetation directly related to human action”.

There are caveats to our questioning of long-term *in situ* refugia for *M. communis*. Specifically, reports that fleshy-fruited myrtle berries are mainly dispersed by frugivorous birds (Herrera, 1984; Traveset, Riera, & Mas, 2001; Gonzalez-Varo, 2010) are consistent with an active role for migration. Moreover, widespread plastid DNA haplotypes and ribotypes (Figure S6) suggest episodes of frequent and/or long-distance migrations of *M. communis* in the western and central parts of the Mediterranean Basin. Our analyses revealed that migrations have been less pronounced in the eastern Mediterranean. Genetic data also suggest that migrations occurred rapidly, recently, and/or over long distances to prevent molecular divergence between remote sites (e.g. the CM genetic cluster).

The phylogeography of *Smilax aspera* L., a climbing plant with sclerophyllous leaves and red berries dispersed by birds, is also congruent with the pattern described for *M. communis* with a longitudinal rather than a latitudinal structure of genetic diversity (Chen *et al.*, 2014). Such a longitudinal organization of phylogroups more or less isolated, but rarely totally disjunct constitutes thus one major phylogeographical trend of the circum-Mediterranean woody species (see the review of Nieto Feliner, 2014). As for *M. communis*, the phylogeography of *Erica arborea* (Désamoré *et al.*, 2011), *Arbutus unedo* (Santiso *et al.*, 2016), and *Laurus nobilis* (Rodriguez-Sanchez *et al.* 2009) support a stronger diversification within the western Mediterranean, and inferred eastward migrations for *Myrtus* and *Arbutus* (see Santiso *et al.*, 2016).

CONCLUSION

Documentation of past range dynamics of Mediterranean woody taxa supports the idea that glaciations led to significant changes in Mediterranean vegetation, such as in the abundance of most thermophilous plants. Our results are in accordance with recent findings indicating that the Mediterranean Basin was less stable from a palaeoenvironmental point of view, having experienced higher extinction rates of species and lineages compared to other Mediterranean-type-ecosystems (Valente & Vargas, 2013; Cowling *et al.*, 2015). *Myrtus communis* is representative of a Tertiary cold-sensitive lineage and we propose here that the severe effects of Pleistocene glaciations were faced despite a relatively reduced role of long-term refugia. *Myrtus communis* seems to have survived the Quaternary glaciations by regional range shifts towards temporary refugia, a response which has, to our knowledge, not been considered in previous Mediterranean phylogeographical or SDM studies. This hypothesis is an important issue regarding conservation or restoration of connectivity between *Myrtus* populations, and more generally between fragments of woodlands to ensure the future resilience of Mediterranean thermophilous shrublands.

ACKNOWLEDGEMENTS

This work was supported by the Provence-Alpes-Côte d'Azur Region, the Conservatoire Botanique National de Corse, and the Conservatoire Botanique National Méditerranéen de Porquerolles. Molecular biology analyses were carried out at the Molecular Biology Common Service of IMBE (Arbois) and the Molecular Biology Platform of INRA URFM (Avignon), with special thanks to Bruno Fady and Anne Roig. We are grateful to Michelle Barbier-Leydet for her help with the European Pollen Database. The English text was edited by Kolo Wamba (Proediting, Redwood City, USA). We thank the numerous contributors to the *Myrtus* sampling, cited in Migliore *et al.* (2012). Finally, we thank the Associate Editor Božo Frajman, Gonzalo Nieto Feliner and another reviewer for their very constructive comments, which helped to improve this manuscript.

REFERENCES

- Ashcroft MB. 2010.** Identifying refugia from climate change. *Journal of Biogeography* **37**: 1407–1413.
- Bandelt HJ, Forster P & Röhl A. 1999.** Median-joining networks for inferring intraspecific phylogenies. *Molecular Biology and Evolution* **16**: 37–48.
- Bennett KD & Provan J. 2008.** What do we mean by ‘refugia’? *Quaternary Science Reviews*: 1–7.
- Besnard G, Khadari B, Navascués M, et al. 2013.** The complex history of the olive tree: from Late Quaternary diversification of Mediterranean lineages to primary domestication in the northern Levant. *Proceedings of the Royal Society B: Biological Sciences* **280**.
- Bonin A, Bellemain E, Bronken Eidesen P, et al. 2004.** How to track and assess genotyping errors in population genetics studies. *Molecular Ecology* **13**: 3261–3273.
- Carnaval AC, Hickerson MJ, Haddad CFB, et al. 2009.** Stability predicts genetic diversity in the Brazilian Atlantic Forest Hotspot. *Science* **323**: 785–789.
- Chen C, Qi ZC, Xu XH, et al. 2014.** Understanding the formation of Mediterranean–African–Asian disjunctions: evidence for Miocene climate-driven vicariance and recent long-distance dispersal in the Tertiary relict *Smilax aspera* (Smilacaceae). *New Phytologist* **204**: 43–255.
- Conchon O. 1986.** Quaternary glaciations in Corsica. *Quaternary Science Reviews* **5**: 429–432.
- Cowling RM, Potts AJ, Bradshaw PL, et al. 2015.** Variation in plant diversity in mediterranean-climate ecosystems: the role of climatic and topographical stability. *Journal of Biogeography* **42**: 552–564.
- Désamoré A, Laenen B, Devos N, et al. 2011.** Out of Africa: north-westwards Pleistocene expansions of the heather *Erica arborea*. *Journal of Biogeography* **38**: 164–176.
- Désamoré A, Laenen B, Gonzalez-Mancebo JM, Jaen Molina R, Bystrakova N, Martinez-Klimova E, Carine MA, Vanderpoorten A. 2012.** Inverted patterns of genetic diversity in continental and island populations of the heather *Erica scoparia* s.l. *Journal of Biogeography* **3**: 574–584.
- Elith J, Graham CH, Anderson RP, et al. 2006.** Novel methods improve prediction of species’ distributions from occurrence data. *Ecography* **29**: 129–151.
- Evanno G, Regnaut S & Goudet J. 2005.** Detecting the number of clusters of individuals using the software STRUCTURE: a simulation study. *Molecular Ecology* **14**: 2611–2620.
- Falush D, Stephens M & Pritchard JK. 2007.** Inference of population structure using multilocus genotype data: dominant markers and null alleles. *Molecular Ecology Notes* **7**: 574–578.
- Fernandez-Mazuecos M & Vargas P. 2010.** Ecological rather than geographical isolation dominates Quaternary formation of Mediterranean *Cistus* species. *Molecular Ecology* **19**: 1381–1395.
- García-Castaño JL, Terrab A, Ortiz MÁ, et al. 2014.** Patterns of phylogeography and vicariance of *Chamaerops humilis* L. (Palmae). *Turkish Journal of Botany* **38**: 1132–1146.

- Gavin DG, Fitzpatrick MC, Gugger PF, et al. 2014.** Climate refugia: joint inference from fossil records, species distribution models and phylogeography. *New Phytologist* **204**: 37–54.
- Guzmán B, Fedriani JM, Delibes M, et al. 2017.** The colonization history of the Mediterranean dwarf palm (*Chamaerops humilis* L., Palmae). *Tree Genetics & Genomes* **13**: 24.
- Gonzalez-Varo JP. 2010.** Fragmentation, habitat composition and the dispersal/predation balance in interactions between the Mediterranean myrtle and avian frugivores. *Ecography* **33**: 185–197.
- González-Varo JP, Albaladejo RG, Aizen MA, et al. 2015.** Extinction debt of a common shrub in a fragmented landscape. *Journal of Applied Ecology* **52**: 580–589.
- González-Varo JP, Arroyo J & Aparicio A. 2009.** Effects of fragmentation on pollinator assemblage, pollen limitation and seed production of Mediterranean myrtle (*Myrtus communis*). *Biological Conservation* **142**: 1058–1065.
- Hampe A, Rodriguez-Sanchez F, Dobrowski S, et al. 2013.** Climate refugia: from the Last Glacial Maximum to the twenty-first century. *New Phytologist* **197**: 16–18.
- Herrera CM. 1984.** A study of avian frugivores, bird-dispersed plants, and their interaction in Mediterranean scrublands. *Ecological Monographs* **54**: 1–23.
- Hijmans RJ, Cameron SE, Parra JL, et al. 2005.** Very High resolution interpolated climate surfaces for global land areas. *International Journal of Climatology* **25**: 1965–1978.
- Mateu-Andrés I, Ciurana MJ, Aguilera A, et al. 2015.** Plastid DNA Homogeneity in *Celtis australis* L. (Cannabaceae) and *Nerium oleander* L. (Apocynaceae) throughout the Mediterranean Basin. *International Journal of Plant Sciences* **176**: 421–432.
- Médail F & Diadema K. 2009.** Glacial refugia influence plant diversity patterns in the Mediterranean Basin. *Journal of Biogeography* **36**: 1333–1345.
- Meineri E & Hylander K. 2017.** Fine-grain, large-domain climate models based on climate station and comprehensive topographic information improve microrefugia detection. *Ecography* **40**: 1003–1013.
- Migliore J, Baumel A, Juin M, et al. 2011.** Genetic diversity and structure of a Mediterranean endemic plant in Corsica (*Mercurialis corsica*, Euphorbiaceae). *Population Ecology* **53**: 573–586.
- Migliore J, Baumel A, Juin M, et al. 2012.** From Mediterranean shores to central Saharan mountains: key phylogeographical insights from the genus *Myrtus*. *Journal of Biogeography* **39**: 942–956.
- Nieto Feliner G. 2014.** Patterns and processes in plant phylogeography in the Mediterranean Basin. A review. *Perspectives in Plant Ecology, Evolution and Systematics*, **16**, 265–278.
- Nikolić T. 2015.** *Myrtus communis* distribution in Croatia. Flora Croatica Database (<http://hirc.botanic.hr/fcd>). Faculty of Science, University of Zagreb (accessed date: 01/2015).

- Nogués-Bravo D. 2009.** Predicting the past distribution of species climatic niches. *Global Ecology and Biogeography* **18**: 521–531.
- Nora S, Albaladejo RG & Aparicio A. 2015.** Genetic variation and structure in the Mediterranean shrubs *Myrtus communis* and *Pistacia lentiscus* in different landscape contexts. *Plant Biology* **17**: 311–319.
- O’Donnell MS, Ignizio DA. 2012.** USGS Data Series 691: Bioclimatic Predictors for Supporting Ecological Applications in the Conterminous United States.
- Otto-Bliesner BL, Marshall SJ, Overpeck JT, et al. 2006.** Simulating Arctic climate warmth and icefield retreat in the Last Interglaciation. *Science* **311**: 1751–1753.
- Peakall R & Smouse PE. 2012.** GENALEX 6.5: genetic analysis in Excel. Population genetic software for teaching and research—an update. *Bioinformatics* **28**: 2537–2539.
- Pearson RG, Raxworthy CJ, Nakamura M, et al. 2007.** Predicting species distributions from small numbers of occurrence records: a test case using cryptic geckos in Madagascar. *Journal of Biogeography* **34**: 102–117.
- Phillips SJ, Anderson RP & Schapire RE. 2006.** Maximum entropy modeling of species geographic distributions. *Ecological Modelling* **190**: 231–259.
- Phillips SJ & Dudík M. 2008.** Modeling of species distributions with MAXENT: new extensions and a comprehensive evaluation. *Ecography* **31**: 161–175.
- Phillips SJ, Anderson RP, Dudík M, Schapire RE & Blair M. 2017.** Opening the black box: an open-source release of MAXENT. *Ecography* **40**: 887–893.
- Pirazzoli PA. 2005.** A review of possible eustatic, isostatic and tectonic contributions in eight late-Holocene relative sea-level histories from the Mediterranean area. *Quaternary Science Reviews* **24**: 1989–2001.
- Postigo Mijarra JM, Barron E, Gomez Manzaneque F, et al. 2009.** Floristic changes in the Iberian Peninsula and Balearic Islands (south-west Europe) during the Cenozoic. *Journal of Biogeography* **36**: 2025–2043.
- Pritchard JK, Stephens M & Donnelly P. 2000.** Inference of population structure using multilocus genotype data. *Genetics* **155**.
- Quézel P & Médail F. 2003.** Ecologie et biogéographie des forêts du bassin méditerranéen. *Elsevier (Collection Environnement) Paris*: 573.
- Ramón-Laca L & Mabberley DJ. 2004.** The ecological status of the carob-tree (*Ceratonia siliqua*, Leguminosae) in the Mediterranean. *Botanical Journal of the Linnean Society* **144**: 431–436.
- Reille M. 1977.** Quelques aspects de l’activité humaine en Corse durant le Subatlantique et ses conséquences sur la végétation. ‘*Approche écologique de l’homme fossile*’ *Supplément au Bulletin de l’AFEQ* **47**: 329–342.

- Reille M. 1984.** Origine de la végétation actuelle de la Corse sud-orientale; analyse pollinique de cinq marais côtiers. *Pollen et spores*.
- Reille M. 1992.** New pollen- analytical researches in Corsica: the problem of *Quercus ilex* L. and *Erica arborea* L., the origin of *Pinus halepensis* Miller forests. *New Phytologist* **122**: 359–378.
- Vella M-A. 2010.** *Approches géomorphologique et géophysique des interactions sociétés/milieus en Corse au cours de l'Holocène*. PhD Thesis, Université de Corte, France.
- Rodríguez-Sánchez F, Arroyo J. 2008.** Reconstructing the demise of Tethyan plants: climate-driven range dynamics of *Laurus* since the Pliocene. *Global Ecology and Biogeography* **17**: 685–695.
- Rodríguez-Sánchez F, Guzman B, Valido A, et al. 2009.** Late Neogene history of the laurel tree (*Laurus* L., Lauraceae) based on phylogeographical analyses of Mediterranean and Macaronesian populations. *Journal of Biogeography* **36**: 1270–1281.
- Rodríguez-Sánchez F, Hampe A, Jordano P, et al. 2010.** Past tree range dynamics in the Iberian Peninsula inferred through phylogeography and palaeodistribution modelling: A review. *Review of Palaeobotany and Palynology* **162**: 507–521.
- Rundel PW, Arroyo MTK, Cowling RM, et al. 2016.** Mediterranean biomes: evolution of their vegetation, floras, and climate. *Annual Review of Ecology, Evolution, and Systematics* **47**: 383–407.
- Santiso X, Lopez L, Retuerto R, et al. 2016.** Phylogeography of a widespread species: pre-glacial vicariance, refugia, occasional blocking straits and long-distance migrations. *AoB PLANTS* **8**.
- Serra-Diaz JM, Scheller RM, Syphard AD, et al. 2015.** Disturbance and climate microrefugia mediate tree range shifts during climate change. *Landscape Ecology* **30**: 1039–1053.
- Stewart JR & Lister AM. 2001.** Cryptic northern refugia and the origins of the modern biota. *Trends in Ecology and Evolution* **16**: 608–613.
- Stewart JR, Lister AM, Barnes I, et al. 2010.** Refugia revisited: individualistic responses of species in space and time. *Proceedings of the Royal Society B Biological Sciences* **277**: 661–671.
- Svenning JC, Fløjgaard C, Marske KA, et al. 2011.** Applications of species distribution modeling to paleobiology. *Quaternary Science Reviews* **30**: 2930–2947.
- Thompson JD. 2005.** *Plant evolution in the Mediterranean*. New York: Oxford University Press.
- Traveset A, Riera N & Mas RE. 2001.** Ecology of fruit-colour polymorphism in *Myrtus communis* and differential effects of birds and mammals on seed germination and seedling growth. *Journal of Ecology* **89**: 749–760.
- Valente LM & Vargas P. 2013.** Contrasting evolutionary hypotheses between two mediterranean-climate floristic hotspots: the Cape of southern Africa and the Mediterranean Basin. *Journal of Biogeography* **40**: 2032–2046.
- Valiente-Banuet A, Rumebe AV, Verdu M, et al. 2006.** Modern Quaternary plant lineages promote diversity through facilitation of ancient Tertiary lineages. *PNAS* **103**: 16812–16817.

- Vargas P, Fernández-Mazuecos M & Heleno R. 2018.** Phylogenetic evidence for a Miocene origin of Mediterranean lineages: species diversity, reproductive traits and geographical isolation. *Plant Biology* **20**: 157–165.
- Vendramin GG, Fady B, González-Martínez SC, et al. 2008.** Genetically depauperate but widespread: the case of an emblematic Mediterranean Pine. *Evolution* **62**: 680–688.
- Vos P, Hogers R, Bleeker M, et al. 1995.** AFLP: a new technique for DNA fingerprinting. *Nucleic Acids Research* **23**: 4407–4414.
- Waltari E, Hijmans RJ, Peterson AT, et al. 2007.** Locating Pleistocene refugia: comparing phylogeographic and ecological niche model predictions. *PLoS ONE* **2**.
- Wu H, Guiot J, Brewer S, et al. 2007.** Climatic changes in Eurasia and Africa at the last glacial maximum and mid-Holocene: reconstruction from pollen data using inverse vegetation modelling. *Climate Dynamics* **29**: 211–229.
- Yackulic CB, Chandler R, Zipkin EF, et al. 2013.** Presence-only modelling using MAXENT: when can we trust the inferences? *Methods in Ecology and Evolution* **4**: 236–243.

**Surviving to glaciations in the Mediterranean region:
an alternative to the long-term refugia hypothesis**

JÉRÉMY MIGLIORE^{1,2*}, ALEX BAUMEL¹, AGATHE LERICHE¹, MARIANICK JUIN¹ and FRÉDÉRIC MÉDAIL¹

¹*Aix Marseille Univ, Avignon Université, CNRS, IRD, Institut Méditerranéen de Biodiversité et d'Ecologie marine et continentale (IMBE), Aix-en-Provence, France.*

²*Current address: Université Libre de Bruxelles, Evolutionary Biology and Ecology, Faculté des Sciences, CP160/12, 1050 Bruxelles, Belgium.*

*Corresponding author. E-mail: jeremy.migliore@imbe.fr / migliore.jeremy@libertysurf.fr

The following Supporting Information is available for this article:

Figure S1. Palaeodistribution of *Myrtus communis* during the LIG and LGM.

MAXENT projection of the model of current distribution of *Myrtus communis* during the Last Inter-Glacial period (ca. 116-130 ka BP) (A), and the Last Glacial Maximum (ca. 19-26.5 ka BP) according to the CCSM4 (B), MIROC-ESM (C) and MPI-ESM-P (D) climate models.

Figure S2. Presence/absence of *Myrtus communis* during the LIG and LGM.

Potential distribution of *Myrtus communis* fitted to current climatic conditions from actual occurrences using MAXENT and projected during the Last Inter-Glacial period (A), and the Last Glacial Maximum using the CCSM4 (B), MIROC-ESM (C) and MPI-ESM-P (D) climate models. Continuous suitability values modelled with MAXENT were converted into presence/absence, using the ten percentile threshold method (see Methods). Shades referred to palaeodistributions modelled just before the chronozone represented.

Figure S3. Palaeodistribution of *Myrtus communis* during the Mid-Holocene.

MAXENT projection of the model of current distribution of *Myrtus communis* during the Mid-Holocene (ca. 6 ka BP) according to the CCSM4 (A), MIROC-ESM (B) and MPI-ESM-P (C) climate models, and during the Present (D).

Figure S4. Presence/absence of *Myrtus communis* during the Mid-Holocene.

Potential distribution of *Myrtus communis* fitted to current climatic conditions from actual occurrences using MAXENT and projected during the Mid-Holocene using the CCSM4 (A), MIROC-ESM (B) and MPI-ESM-P (C) climate models, and during the Present (D). Continuous suitability values modelled with MAXENT were converted into presence/absence, using the ten percentile threshold method (see Methods). Shades referred to palaeodistributions modelled just before the chronozone represented.

Figure S5. Analysis of STRUCTURE results for AFLP data.

Representation of the Log probability of data L(K) (A) and the magnitude of ΔK (B) as a function of K for the AFLP dataset of *Myrtus communis*, according to Evanno *et al.* (2005) and the software STRUCTUREHARVESTER (Earl *et al.*, 2012).

Figure S6. Spatial genetic structure with haplotypes identifiers of *Myrtus communis*, based on plastid DNA and nuclear DNA.

Spatial genetic structure with haplotypes identifiers of *Myrtus communis* through its Mediterranean distribution range, based on the median-joining networks from plastid DNA sequences *trnL-trnF* and *rpl2-trnH* intergenic regions (A,C) and nuclear DNA sequences external transcribed spacer (ETS) region and internal transcribed spacer (ITS1-5.8S-ITS2) (B,D). When more than one individual was sequenced per population circles on the maps are horizontally divided in two, and if spatially-closed populations have the same haplotypes or ribotypes they are separated by the symbol "/". Circle sizes in networks are proportional to haplotype/ribotype frequencies.

Table S1. List of samples of *Myrtus communis* used for genetic analyses (plastid and nuclear sequencing, and AFLP genotyping).

Table S2. AIC scores and number of parameters for fitted MAXENT models.

Akaike Information Criterion (AIC) scores and number of parameters for all fitted MAXENT models using all possible simple and combination of features except "threshold": L = linear, Q = quadratic, P = product.

Table S3. Bibliographic review of the main imprints left by past environmental changes on Mediterranean widespread, Tertiary-originated, and/or thermophilous woody species, combining genetic, distribution modelling and palaeoecological data.

Bibliographic review of the main imprints left by past environmental changes on Mediterranean widespread, Tertiary-originated, and/or thermophilous woody species, combining genetic, distribution modelling and palaeoecological data. Mean values of cold resistance for vegetative organs in adult specimens are those causing 50% damage to leaf buds and cambium (based on Larcher, 1981, 2000; Quézel & Médail, 2003; Flexas *et al.*, 2014).

Figure S1. Palaeodistribution of *Myrtus communis* during the LIG and LGM.

MAXENT projection of the model of current distribution of *Myrtus communis* during the Last Inter-Glacial period (ca. 116-130 ka BP) (A), and the Last Glacial Maximum (ca. 19-26.5 ka BP) according to the CCSM4 (B), MIROC-ESM (C) and MPI-ESM-P (D) climate models.

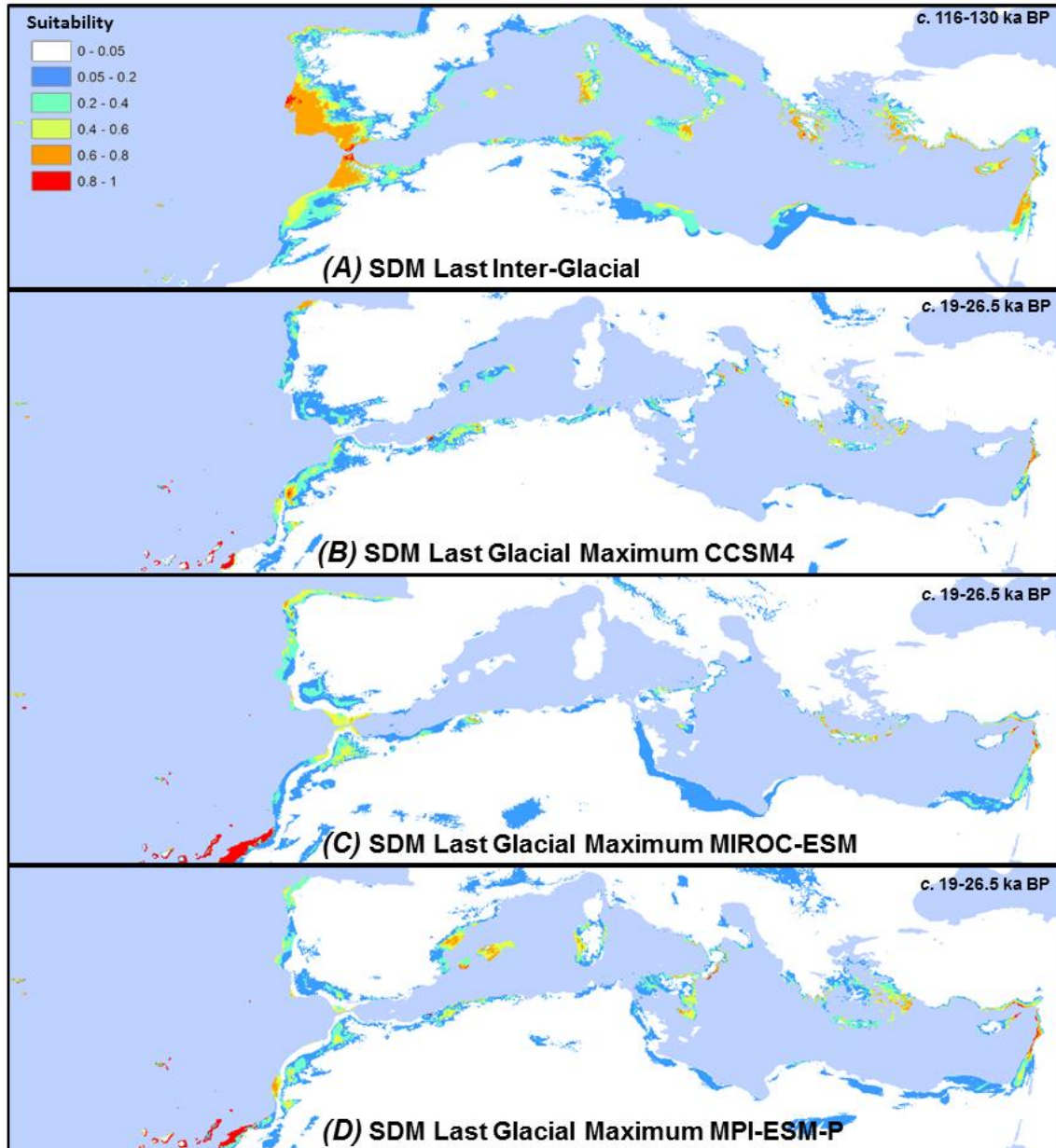


Figure S2. Presence/absence of *Myrtus communis* during the LIG and LGM.

Potential distribution of *Myrtus communis* fitted to current climatic conditions from actual occurrences using MAXENT and projected during the Last Inter-Glacial period (A), and the Last Glacial Maximum using the CCSM4 (B), MIROC-ESM (C) and MPI-ESM-P (D) climate models. Continuous suitability values modelled with MAXENT were converted into presence/absence, using the ten percentile threshold method (see Methods). Shades referred to palaeodistributions modelled just before the chronozone represented.

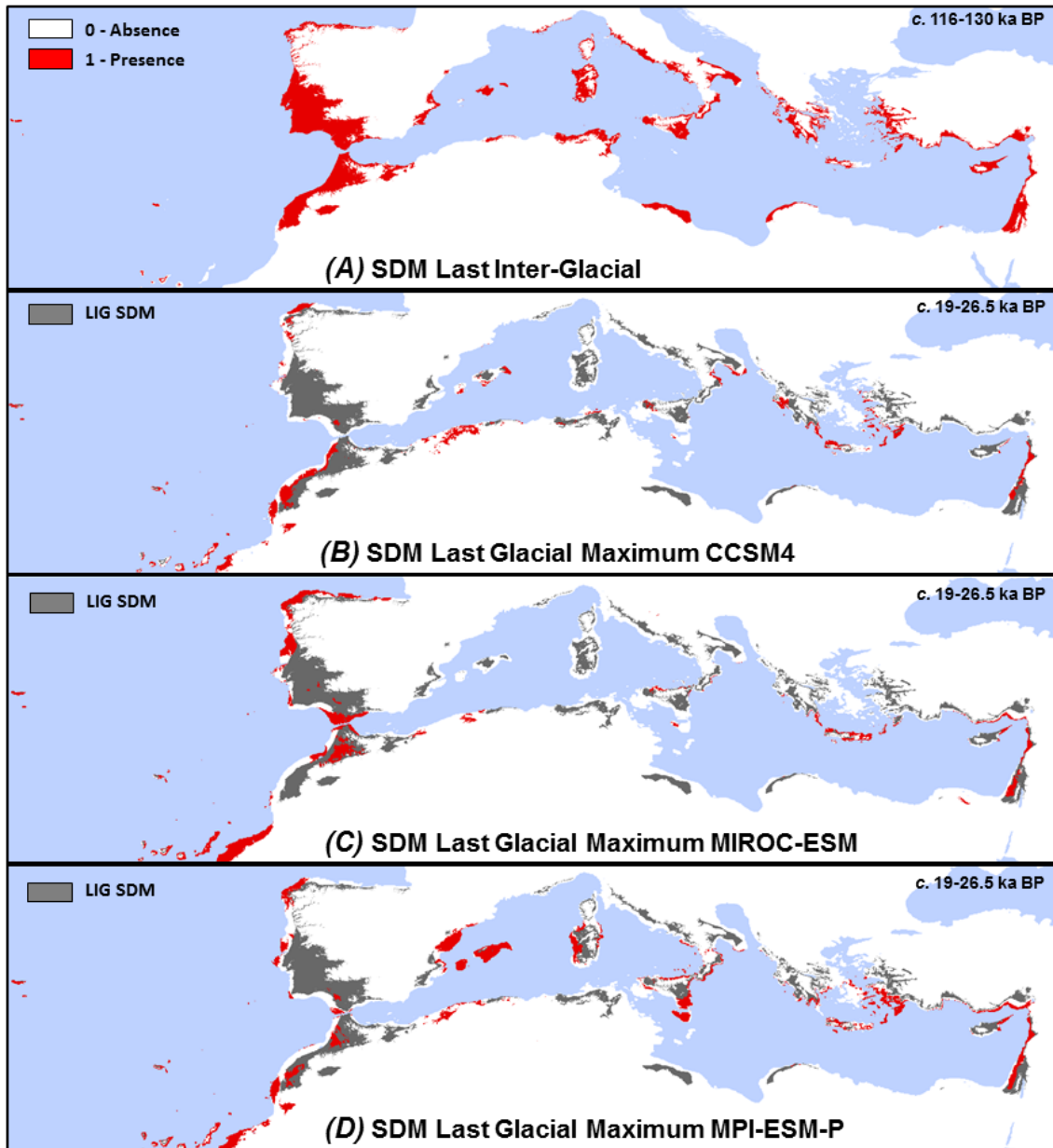


Figure S3. Palaeodistribution of *Myrtus communis* during the Mid-Holocene.

MAXENT projection of the model of current distribution of *Myrtus communis* during the Mid-Holocene (*ca.* 6 ka BP) according to the CCSM4 (A), MIROC-ESM (B) and MPI-ESM-P (C) climate models, and during the Present (D).

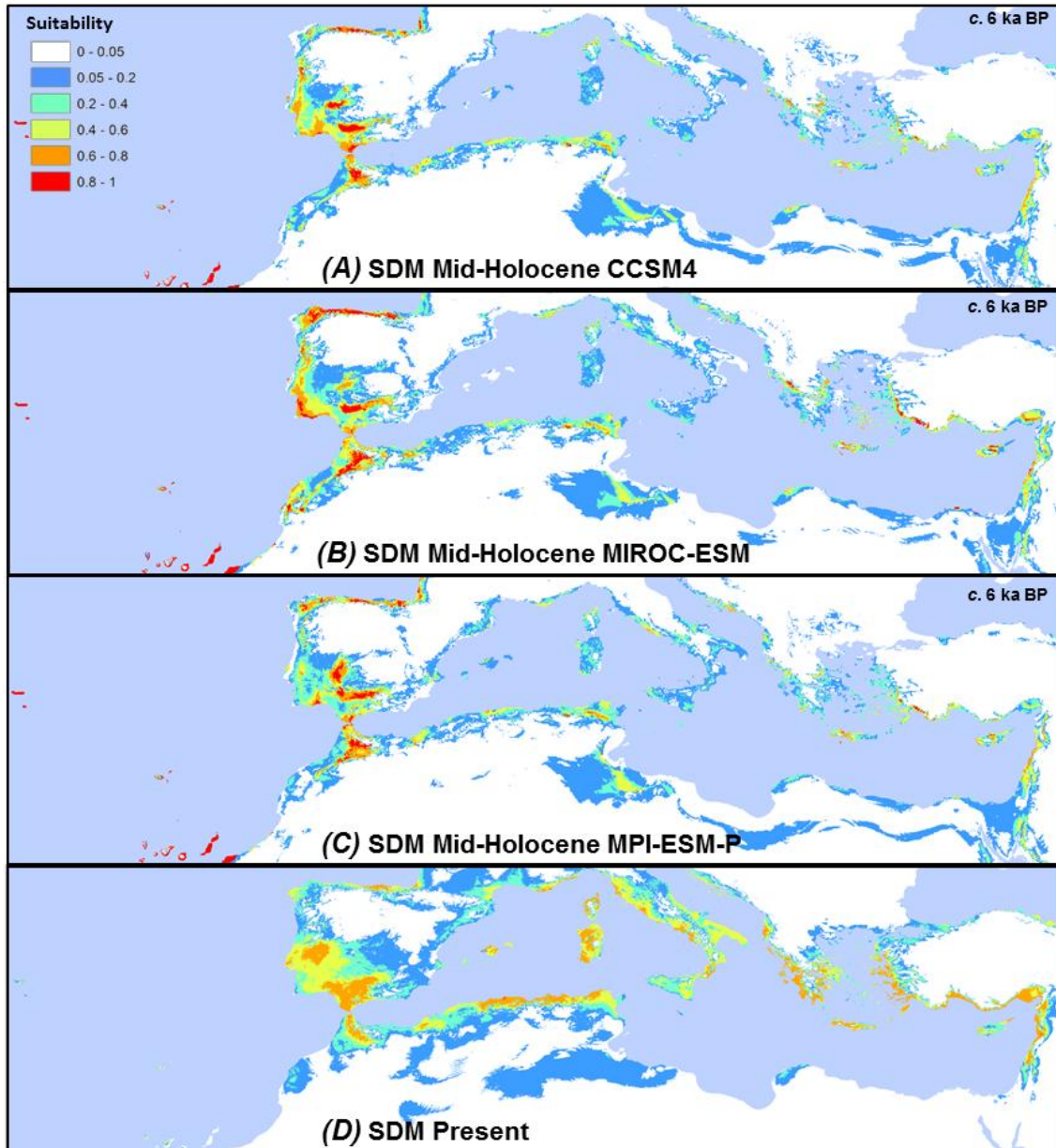


Figure S4. Presence/absence of *Myrtus communis* during the Mid-Holocene.

Potential distribution of *Myrtus communis* fitted to current climatic conditions from actual occurrences using MAXENT and projected during the Mid-Holocene using the CCSM4 (A), MIROC-ESM (B) and MPI-ESM-P (C) climate models, and during the Present (D). Continuous suitability values modelled with MAXENT were converted into presence/absence, using the ten percentile threshold method (see Methods). Shades referred to palaeodistributions modelled just before the chronozone represented.

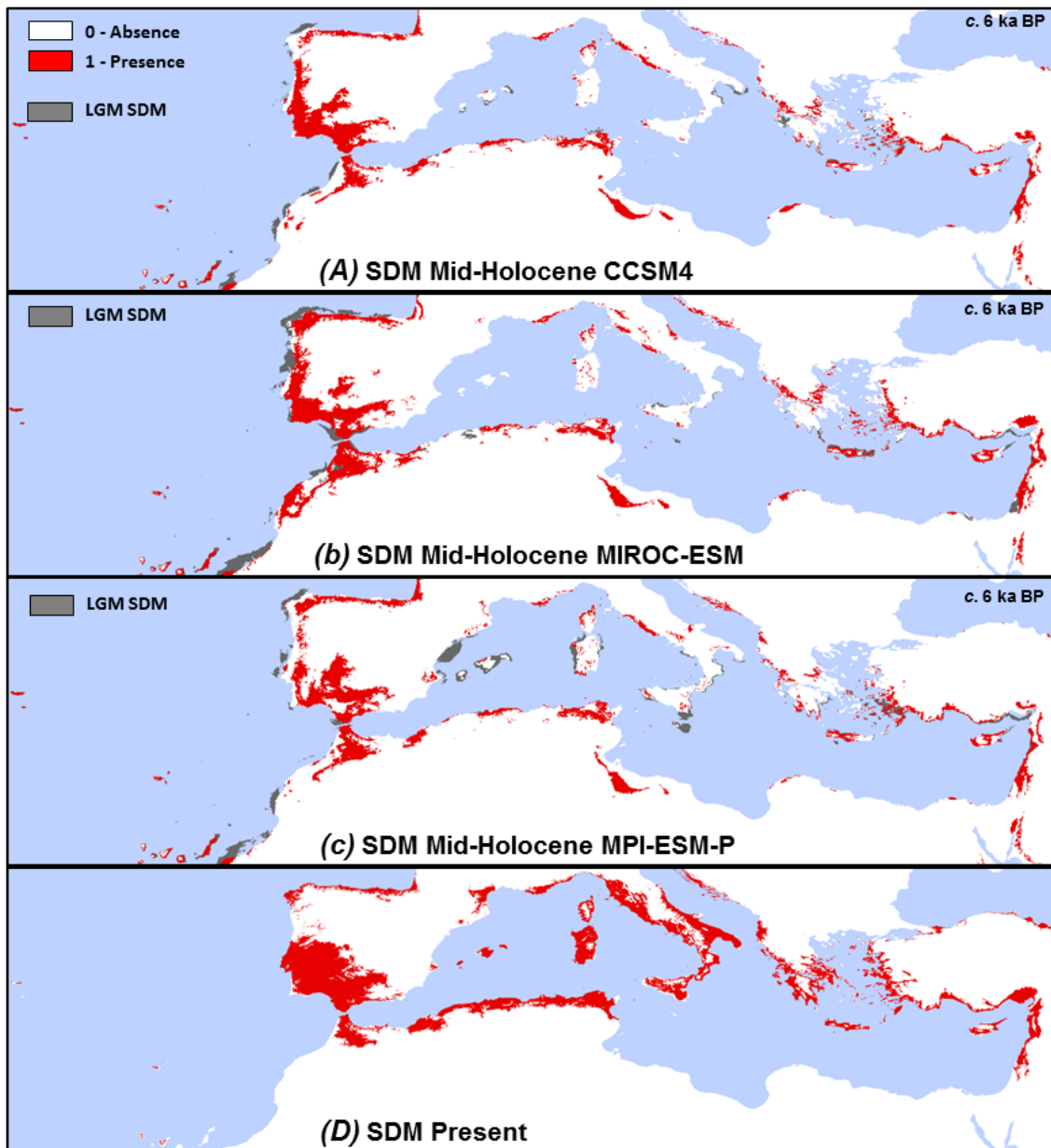


Figure S5. Analysis of *STRUCTURE* results for AFLP data.

Representation of the Log probability of data $L(K)$ (A) and the magnitude of ΔK (B) as a function of K for the AFLP dataset of *Myrtus communis*, according to Evanno *et al.* (2005) and the software STRUCTUREHARVESTER (Earl *et al.*, 2012).

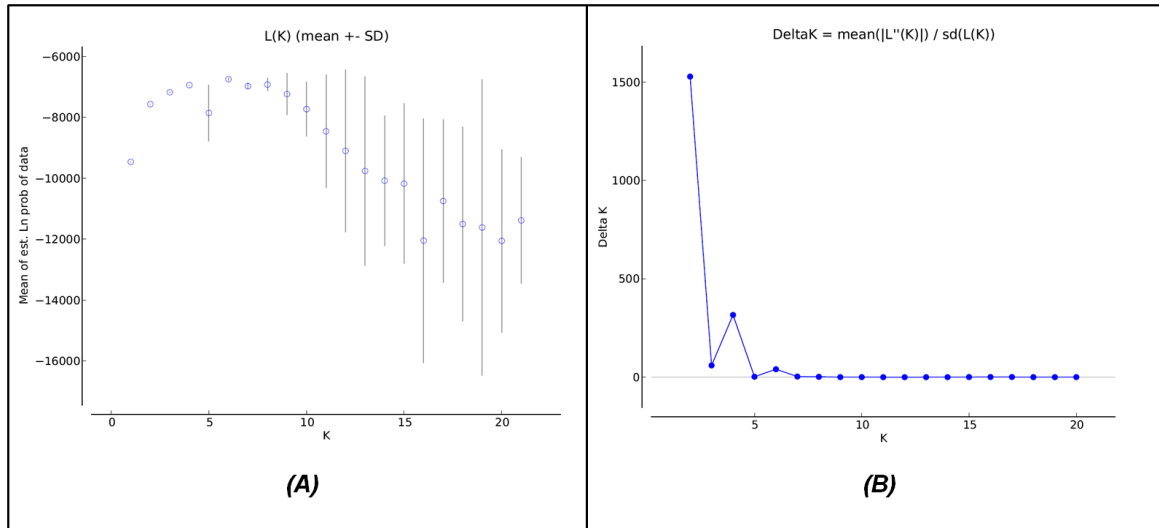
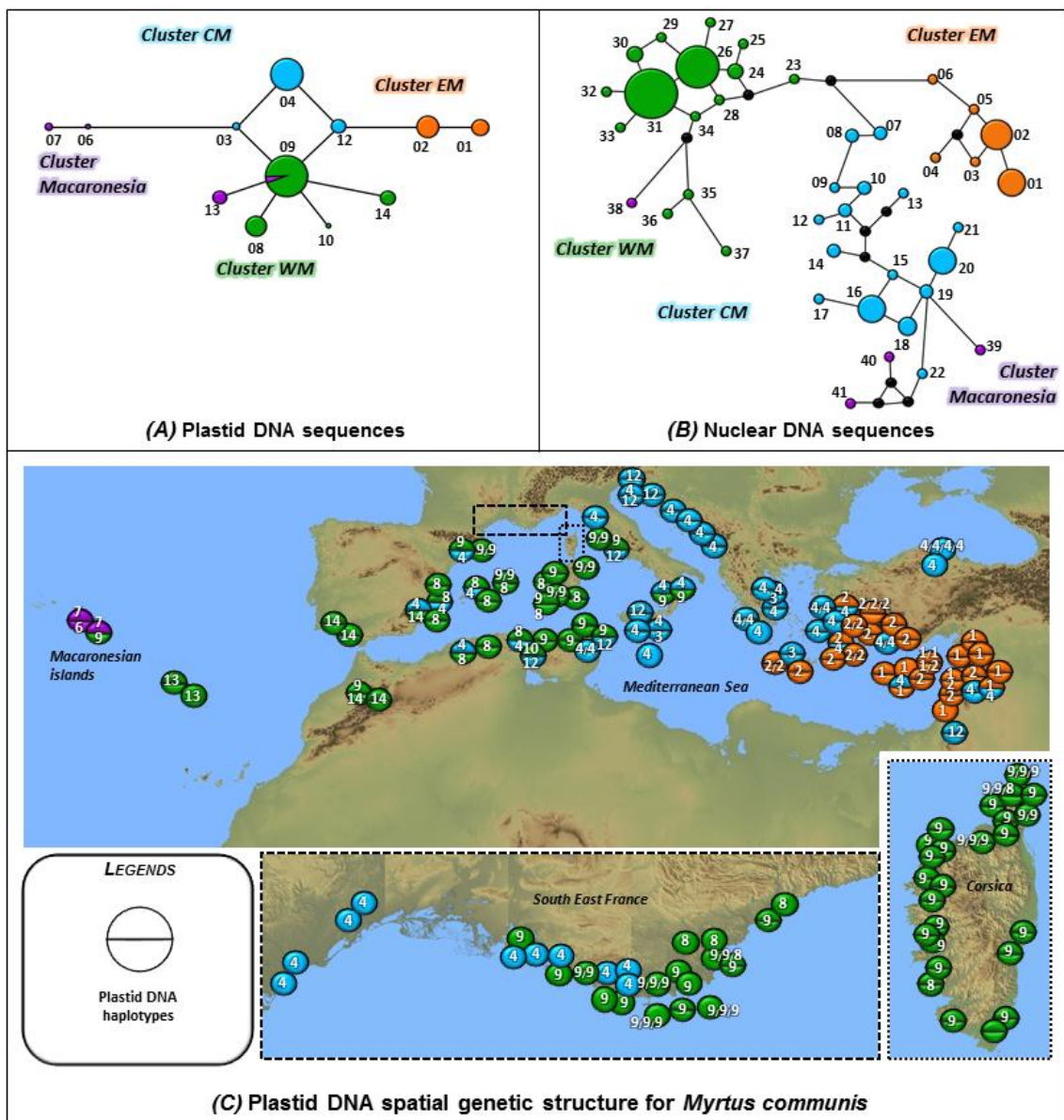


Figure S6. Spatial genetic structure with haplotypes identifiers of *Myrtus communis*, based on plastid DNA and nuclear DNA.

Spatial genetic structure with haplotypes identifiers of *Myrtus communis* through its Mediterranean distribution range, based on the median-joining networks from plastid DNA sequences *trnL-trnF* and *rpl2-trnH* intergenic regions (A,C) and nuclear DNA sequences external transcribed spacer (ETS) region and internal transcribed spacer (ITS1-5.8S-ITS2) (B,D). When more than one individual was sequenced per population circles on the maps are horizontally divided in two, and if spatially-closed populations have the same haplotypes or ribotypes they are separated by the symbol “/”. Circle sizes in networks are proportional to haplotype/ribotype frequencies.



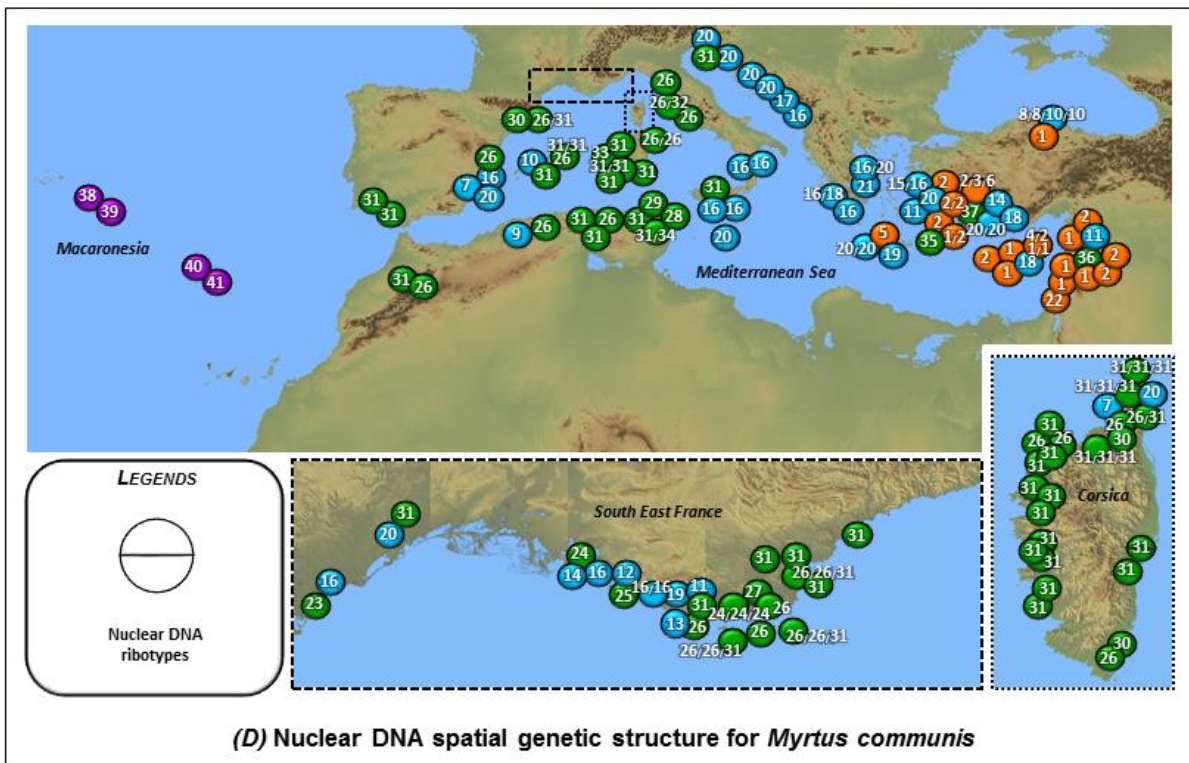


Table S1. List of samples of *Myrtus communis* used for genetic analyses (plastid and nuclear sequencing, and AFLP genotyping).

Samples	Locations	X	Y	AFLP clusters	Plastid DNA haplotypes	GenBank <i>trnL-trnF</i>	GenBank <i>rpl2-trnH</i>	Nuclear DNA ribotypes	GenBank ITS1-5,8S-ITS2	GenBank ETS-18S
ALBA1	Albania	19.483458	40.98658	CM	4	FJ611337	HM014154	16	GU984346	HM106407
ALBA9	Albania	19.483458	40.98658	/	4	FJ611337	HM014154	/	/	/
ABEJ1	Algeria	4.98194444	36.80777778	/	8	FJ611338	HM014153	31	JF304836	JF304896
ABEJ5	Algeria	4.98194444	36.80777778	WM	4	FJ611337	HM014154	/	/	/
AKED1	Algeria	3.447559	36.633195	/	8	FJ611338	HM014153	26	GU984342	JF304896
AKED9	Algeria	3.447559	36.633195	/	8	FJ611338	HM014153	/	/	/
ANAB1	Algeria	7.730648	36.924454	/	9	FJ611338	HM014149	26	GU984342	HM106410
ANAB9	Algeria	7.730648	36.924454	WM	9	FJ611338	HM014149		/	/
AOTE1	Algeria	8.61805556	36.88611111	WM	9	FJ611338	HM014149	31	GU984340	JF304871
AOTE5	Algeria	8.61805556	36.88611111	/	9	FJ611338	HM014149	/	/	/
ASKI1	Algeria	6.913462	36.849758	/	12	FJ611337	HM014149	31	GU984340	JF304896
ASKI9	Algeria	6.913462	36.849758	WM	10	FJ611338	HM014152	/	/	/
ATIP1	Algeria	2.48250000	36.69055556	/	4	FJ611337	HM014154	9	JF304815	JF304895
ATIP5	Algeria	2.48250000	36.69055556	WM	8	FJ611338	HM014153	/	/	/
CRBA1	Croatia	13.759879	44.915334	CM	4	FJ611337	HM014154	31	JF304826	JF304897
CRBA5	Croatia	13.759879	44.915334	/	12	FJ611337	HM014149	/	/	/
CRBB1	Croatia	13.765167	44.913663	/	12	FJ611337	HM014149	20	JF304843	HM106406
CRBB5	Croatia	13.765167	44.913663	/	12	FJ611337	HM014149	/	/	/
CRBC1	Croatia	13.762508	44.910714	/	12	FJ611337	HM014149	20	JF304844	JF304884
CRBC5	Croatia	13.762508	44.910714	/	12	FJ611337	HM014149	/	/	/
CRDU1	Croatia	14.83429	44.14579	/	4	FJ611337	HM014154	20	GU984343	HM106406
CRDU5	Croatia	14.83429	44.14579	CM	4	FJ611337	HM014154	/	/	/
CRKO1	Croatia	17.04223	43.28286	/	4	FJ611337	HM014154	17	JF304852	JF304876
CRKO5	Croatia	17.04223	43.28286	CM	4	FJ611337	HM014154	/	/	/
CRLE1	Croatia	15.233333	43.831111	/	4	FJ611337	HM014154	20	JF304845	HM106406
CRLE9	Croatia	15.233333	43.831111	CM	4	FJ611337	HM014154	/	/	/
CAKB1	Cyprus	32.950222	34.590694	/	4	FJ611337	HM014154	1	JF304857	HM106405

CAKB9	Cyprus	32.950222	34.590694	/	1	FJ611337	HM014156	/	/	/
CAKC1	Cyprus	32.944028	34.596639	/	1	FJ611337	HM014156	1	GU984349	HM106405
CAKR1	Cyprus	32.971111	34.6005	EM	2	FJ611337	HM14157	18	JF304849	HM106407
CAKR9	Cyprus	32.971111	34.6005	/	2	FJ611337	HM14157	/	/	/
CLYS1	Cyprus	32.56634000	35.00402200	/	1	FJ611337	HM014156	2	JF304858	JF304877
CLYS6	Cyprus	32.56634000	35.00402200	CM	1	FJ611337	HM014156	/	/	/
CPAF1	Cyprus	32.60440100	34.94194800	/	1	FJ611337	HM014156	2	GU984350	HM106405
CPAF7	Cyprus	32.60440100	34.94194800	EM	1	FJ611337	HM014156	/	/	/
CTRO1	Cyprus	32.83269000	34.91617900	/	1	FJ611337	HM014156	4	GU984351	JF304885
CTRO9	Cyprus	32.83269000	34.91617900	EM	1	FJ611337	HM014156	/	/	/
CXYL1	Cyprus	33.03866400	35.00752100	/	1	FJ611337	HM014156	1	JF304818	HM106405
CXYL5	Cyprus	33.03866400	35.00752100	EM	1	FJ611337	HM014156	/	/	/
CYIA1	Cyprus	32.52331700	35.09252500	/	2	FJ611337	HM14157	1	JF304818	JF304877
CYIA9	Cyprus	32.52331700	35.09252500	EM	2	FJ611337	HM14157	/	/	/
FANT1	France	7.13218	43.564051	/	9	FJ611338	HM014149	31	GU984340	HM106410
FANT6	France	7.13218	43.564051	/	9	FJ611338	HM014149	/	/	/
FAUZ1	France	3.09650000	43.13469444	/	4	FJ611337	HM014154	23	GU984356	JF304887
FBAG1	France	6.36269200	43.01325600	/	9	FJ611338	HM014149	26	GU984342	HM106410
FBAG9	France	6.36269200	43.01325600	/	9	FJ611338	HM014149	/	/	/
FBAT1	France	5.94361111	43.68416667	/	9	FJ611338	HM014149	26	GU984342	HM106410
FBER1	France	6.29772222	43.16180556	/	9	FJ611338	HM014149	24	JF304865	HM106410
FBLA1	France	6.655833	43.514722	/	8	FJ611338	HM014153	31	GU984340	JF304896
FCAS1	France	5.77444444	43.19744444	/	4	FJ611337	HM014154	19	GU984344	JF304886
FCAV1	France	6.41998800	43.16439000	/	9	FJ611338	HM014149	27	GU984342	JF304896
FCEM9	France	6.39295700	43.00514800	/	9	FJ611338	HM014149	31	JF304840	HM106410
FCLA1	France	6.37194444	43.14555556	/	9	FJ611338	HM014149	24	GU984359	JF304896
FCPA12	France	6.384974	43.012266	/	9	FJ611338	HM014149	26	GU984342	HM106410
FCSU4	France	6.381605	43.00709	/	9	FJ611338	HM014149	26	GU984342	HM106410
FCYR1	France	5.75916667	43.18761111	/	9	FJ611338	HM014149	16	GU984346	HM106407
FESC1	France	5.04878823	43.44322673	/	8	FJ611338	HM014153	31	GU984340	HM106410
FFIG1	France	5.04878823	43.44322673	CM	9	FJ611338	HM014149	24	JF304865	HM106410
FGAL1	France	6.95048091	43.49886753	WM	8	FJ611338	HM014153	26	GU984342	HM106410
FGAR1	France	3.81638889	43.52900000	/	4	FJ611337	HM014154	20	GU984343	HM106406

FMAL1	France	5.70861111	43.19891667	/	9	FJ611338	HM014149	16	JF304817	JF304884
FMAR3	France	7.04962200	43.51886200	/	9	FJ611338	HM014149	31	GU984340	HM106410
FMAR7	France	7.04962200	43.51886200	/	9	FJ611338	HM014149	/	/	/
FNAR1	France	4.74138889	43.93086111	/	4	FJ611337	HM014154	31	GU984340	HM106410
FNDA1	France	6.93951872	43.50078637	WM	9	FJ611338	HM014149	31	GU984340	HM106410
FPAG1	France	6.186999	43.004228	/	9	FJ611338	HM014149	26	GU984342	HM106410
FPCO9	France	6.216625	43.007214	/	9	FJ611338	HM014149	31	JF304840	HM106410
FPEY1	France	6.93330136	43.52349017	WM	9	FJ611338	HM014149	26	GU984342	HM106410
FPOC1	France	6.93524569	43.50712009	/	9	FJ611338	HM014149	26	GU984342	JF304899
FPRA1	France	6.45155556	43.15933333	/	9	FJ611338	HM014149	24	JF304865	JF304896
FPSA15	France	6.22675600	42.99911000	/	9	FJ611338	HM014149	26	GU984342	HM106410
FREA1	France	5.931973	43.518862	/	4	FJ611337	HM014154	11	JF304821	JF304869
FREB2	France	5.921137	43.178475	/	4	FJ611337	HM014154	31	GU984340	HM106410
FROQ7	France	7.462141	43.761449	/	8	FJ611338	HM014153	/	/	/
FROU1	France	5.17899984	43.33968554	WM	4	FJ611337	HM014154	16	JF304817	JF304884
FSAU1	France	5.09154350	43.34054369	CM	4	FJ611337	HM014154	14	JF304822	JF304884
FSOU1	France	5.55000000	43.19876111	CM	9	FJ611338	HM014149	25	GU984359	HM106411
FSTA1	France	8.82637600	42.67348100	/	9	FJ611338	HM014149	26	GU984342	HM106410
FSTM1	France	5.91706944	43.07143333	/	9	FJ611338	HM014149	13	GU984366	JF304870
FVAU1	France	5.49916667	43.20611111	CM	4	FJ611337	HM014154	12	JF304864	JF304888
FVER1	France	8.774733	41.813683	/	9	FJ611338	HM014149	31	JF304837	HM106410
FVER9	France	8.774733	41.813683	/	9	FJ611338	HM014149	/	/	/
FVIG1	France	3.11052778	43.14902778	/	4	FJ611337	HM014154	16	GU984346	HM106407
FAGA1	France (Corsica)	9.107883	42.64935	WM	9	FJ611338	HM014149	31	JF304837	HM106410
FAGA9	France (Corsica)	9.107883	42.64935	/	9	FJ611338	HM014149	/	/	/
FAGB2	France (Corsica)	9.161183	42.556533	/	9	FJ611338	HM014149	31	GU984340	HM106410
FAGB9	France (Corsica)	9.161183	42.556533	WM	9	FJ611338	HM014149	/	/	/
FAGH1	France (Corsica)	8.630917	42.249267	WM	9	FJ611338	HM014149	31	JF304837	HM106410
FAGH9	France (Corsica)	8.630917	42.249267	/	9	FJ611338	HM014149	/	/	/
FANG1	France (Corsica)	8.693083	42.40615	WM	9	FJ611338	HM014149	31	GU984340	JF304896

FANG9	France (Corsica)	8.693083	42.40615	/	9	FJ611338	HM014149	/	/	/
FARG1	France (Corsica)	8.679583	42.47105	WM	9	FJ611338	HM014149	31	GU984340	HM106410
FARG9	France (Corsica)	8.679583	42.47105	/	9	FJ611338	HM014149	/	/	/
FARI1	France (Corsica)	9.346317	42.7381	WM	9	FJ611338	HM014149	26	JF304826	JF304886
FARI9	France (Corsica)	9.346317	42.7381	/	9	FJ611338	HM014149	/	/	/
FBAR3	France (Corsica)	9.500233	43.00765	WM	9	FJ611338	HM014149	31	GU984340	HM106410
FBAR9	France (Corsica)	9.500233	43.00765	/	9	FJ611338	HM014149	/	/	/
FCAM2	France (Corsica)	9.423367	42.962217	/	9	FJ611338	HM014149	31	GU984340	HM106410
FCAM5	France (Corsica)	9.423367	42.962217	/	9	FJ611338	HM014149	/	/	/
FCAP1	France (Corsica)	8.721833	42.064183	WM	9	FJ611338	HM014149	31	JF304837	JF304896
FCAP5	France (Corsica)	8.721833	42.064183	/	9	FJ611338	HM014149	/	/	/
FCAR1	France (Corsica)	9.34433333	41.57481389	WM	9	FJ611338	HM014149	30	GU984340	HM106410
FCAR5	France (Corsica)	9.34433333	41.57481389	/	9	FJ611338	HM014149	/	/	/
FCIG1	France (Corsica)	8.720283	41.739583	WM	8	FJ611338	HM014153	31	GU984340	JF304896
FCIG9	France (Corsica)	8.720283	41.739583	/	8	FJ611338	HM014153	/	/	/
FCUC1	France (Corsica)	9.26945	42.627367	WM	9	FJ611338	HM014149	31	GU984340	HM106410
FCUC9	France (Corsica)	9.26945	42.627367	/	9	FJ611338	HM014149	/	/	/
FERB1	France (Corsica)	9.455683	42.756667	WM	9	FJ611338	HM014149	30	GU984372	HM106410
FERB9	France (Corsica)	9.455683	42.756667	/	9	FJ611338	HM014149	/	/	/
FEVE1	France (Corsica)	8.726376	42.573481	/	/	FJ611337	/	26	GU984342	HM106410
FGIO1	France (Corsica)	9.34505	42.8665	/	9	FJ611338	HM014149	31	GU984340	HM106410
FGIO9	France (Corsica)	9.34505	42.8665	/	9	FJ611338	HM014149	/	/	/
FLUC1	France (Corsica)	9.374	42.90895	WM	9	FJ611338	HM014149	31	JF304826	JF304898

FLUC9	France (Corsica)	9.374	42.90895	/	9	FJ611338	HM014149	/	/	/
FLUR3	France (Corsica)	9.560433	42.890167	WM	9	FJ611338	HM014149	26	JF304833	JF304886
FLUR9	France (Corsica)	9.560433	42.890167	/	9	FJ611338	HM014149	/	/	/
FMAC1	France (Corsica)	9.450333	42.968	/	9	FJ611338	HM014149	20	GU984343	HM106406
FMAC5	France (Corsica)	9.450333	42.968	/	9	FJ611338	HM014149	/	/	/
FMUS1	France (Corsica)	9.19558611	41.40493611	WM	9	FJ611338	HM014149	26	GU984342	HM106410
FMUS9	France (Corsica)	9.19558611	41.40493611	/	9	FJ611338	HM014149	/	/	/
FNIC1	France (Corsica)	8.758683	42.0345	WM	9	FJ611338	HM014149	31	GU984340	HM106410
FNIC4	France (Corsica)	8.758683	42.0345	/	9	FJ611338	HM014149	/	/	/
FNON1	France (Corsica)	9.341683	42.8031	/	8	FJ611338	HM014153	31	GU984340	HM106410
FNON9	France (Corsica)	9.341683	42.8031	/	9	FJ611338	HM014149	/	/	/
FOLC1	France (Corsica)	9.36635	42.810033	WM	9	FJ611338	HM014149	7	JF304832	JF304886
FOLC9	France (Corsica)	9.36635	42.810033	/	9	FJ611338	HM014149	/	/	/
FOSC1	France (Corsica)	8.72637600	42.57348100	WM	9	FJ611338	HM014149	31	JF304837	HM106410
FOSC9	France (Corsica)	8.72637600	42.57348100	/	9	FJ611338	HM014149	/	/	/
FPAL1	France (Corsica)	8.664817	42.3667	WM	9	FJ611338	HM014149	31	GU984340	JF304896
FPAL5	France (Corsica)	8.664817	42.3667	/	9	FJ611338	HM014149	/	/	/
FPIE1	France (Corsica)	9.484233	42.83105	/	9	FJ611338	HM014149	31	JF304837	HM106410
FPIE5	France (Corsica)	9.484233	42.83105	/	9	FJ611338	HM014149	/	/	/
FPIN1	France (Corsica)	9.44856	42.03714	/	9	FJ611338	HM014149	31	GU984340	HM106410
FPIN9	France (Corsica)	9.44856	42.03714	/	9	FJ611338	HM014149	31	GU984340	HM106410
FSOB1	France (Corsica)	9.30121667	41.83389444	WM	9	FJ611338	HM014149	31	GU984340	HM106410
FSOB9	France (Corsica)	9.30121667	41.83389444	/	9	FJ611338	HM014149	/	/	/

FTOL1	France (Corsica)	9.384417	43.007983	/	9	FJ611338	HM014149	31	GU984340	JF304896
FTOL9	France (Corsica)	9.384417	43.007983	/	9	FJ611338	HM014149	/	/	/
FTRA1	France (Corsica)	8.70015	42.28985	WM	9	FJ611338	HM014149	31	JF304837	HM106410
FTRA9	France (Corsica)	8.70015	42.28985	/	9	FJ611338	HM014149	/	/	/
FTRI1	France (Corsica)	8.66345	42.106783	WM	9	FJ611338	HM014149	31	JF304837	HM106411
FTRI9	France (Corsica)	8.66345	42.106783	/	9	FJ611338	HM014149	/	/	/
GDEK1	Greece	23.797778	38.15	CM	4	FJ611337	HM014154	21	GU984343	HM106423
GDEK9	Greece	23.797778	38.15	/	4	FJ611337	HM014154	/	/	/
GEUB1	Greece	23.35410000	38.72628333	/	4	FJ611337	HM014154	16	GU984346	HM106407
GEUB5	Greece	23.35410000	38.72628333	CM	3	FJ611338	HM014154	/	/	/
GFRA1	Greece	21.37250000	37.76666700	CM	4	FJ611337	HM014154	18	JF304830	JF304870
GFRA9	Greece	21.37250000	37.76666700	/	4	FJ611337	HM014154	/	/	/
GKAR0	Greece	22.231514	36.893082	CM	4	FJ611337	HM014154	16	GU984346	HM106407
GLOU1	Greece	21.138889	37.871111	CM	4	FJ611337	HM014154	16	JF304847	HM106407
GLOU9	Greece	21.138889	37.871111	/	4	FJ611337	HM014154	/	/	/
GPFL1	Greece	23.20383	39.3679	/	4	FJ611337	HM014154	20	GU984343	HM106406
GPFL9	Greece	23.20383	39.3679	CM	4	FJ611337	HM014154	/	/	/
GCEA1	Greece (Crete)	23.581238	35.499497	CM	2	FJ611337	HM14157	19	JF304847	JF304884
GCEA5	Greece (Crete)	23.581238	35.499497	/	2	FJ611337	HM14157	/	/	/
GCKA1	Greece (Crete)	23.761636	35.52886	CM	3	FJ611338	HM014154	5	JF304859	HM106405
GCKA9	Greece (Crete)	23.761636	35.52886	/	3	FJ611338	HM014154	/	/	/
GCPA1	Greece (Crete)	23.677819	35.23479	CM	2	FJ611337	HM14157	20	GU984343	HM106406
GCPA9	Greece (Crete)	23.677819	35.23479	/	2	FJ611337	HM14157	/	/	/
GCTH1	Greece (Crete)	24.642903	35.258242	CM	2	FJ611337	HM14157	20	GU984343	HM106406
GCTH9	Greece (Crete)	24.642903	35.258242	/	2	FJ611337	HM14157	/	/	/
GREP1	Greece (Rhodes)	28.112613	36.256984	/	2	FJ611337	HM14157	2	JF304828	JF304878
GREP9	Greece	28.112613	36.256984	/	4	FJ611337	HM014154	/	/	/

(Rhodes)										
GRLA1	Greece (Rhodes)	27.94726	36.15648	CM	2	FJ611337	HM14157	2	JF304860	JF304878
GRLA9	Greece (Rhodes)	27.94726	36.15648	/	2	FJ611337	HM14157	/	/	/
GRMO1	Greece (Rhodes)	27.714646	36.124133	CM	2	FJ611337	HM14157	35	GU984364	HM106414
GRMO9	Greece (Rhodes)	27.714646	36.124133	/	2	FJ611337	HM14157	/	/	/
GRPE1	Greece (Rhodes)	28.057702	36.339223	CM	2	FJ611337	HM14157	1	GU984349	JF304879
GRPE9	Greece (Rhodes)	28.057702	36.339223	/	2	FJ611337	HM14157	/	/	/
HCAR0	Israel	35.045817	32.726517	CM	1	FJ611337	HM014156	2	GU984350	JF304878
HHER1	Israel	35.80517200	33.42368600	/	2	FJ611337	HM14157	1	GU984349	JF304878
HHER5	Israel	35.80517200	33.42368600	CM	2	FJ611337	HM14157	/	/	/
IBON1	Italy	15.900045	39.577808	/	9	FJ611338	HM014149	16	GU984346	HM106407
IBON5	Italy	15.900045	39.577808	CM	4	FJ611337	HM014154	/	/	/
ICAS1	Italy	16.259126	39.758471	/	4	FJ611337	HM014154	16	JF304855	HM106407
ICAS5	Italy	16.259126	39.758471	CM	9	FJ611338	HM014149	/	/	/
IMON1	Italy	10.91294444	43.43627778	/	4	FJ611337	HM014154	26	JF304842	HM106410
IMON9	Italy	10.91294444	43.43627778	WM	4	FJ611337	HM014154	/	/	/
ISTI1	Italy	11.14244900	42.92284000	/	9	FJ611338	HM014149	26	GU984342	JF304901
ISTI5	Italy	11.14244900	42.92284000	WM	9	FJ611338	HM014149	/	/	/
IALG3	Italy (Sardinia)	8.36624000	40.53540500	/	9	FJ611338	HM014149	31	JF304837	JF304896
IALG7	Italy (Sardinia)	8.36624000	40.53540500	WM	9	FJ611338	HM014149	/	/	/
IARC1	Italy (Sardinia)	8.870255	39.1611435	WM	9	FJ611338	HM014149	31	GU984340	JF304896
IARC4	Italy (Sardinia)	8.870255	39.1611435	/	9	FJ611338	HM014149	/	/	/
IDOR3	Italy (Sardinia)	9.61492800	40.32195000	/	9	FJ611338	HM014149	26	GU984342	JF304896
IDOR7	Italy (Sardinia)	9.61492800	40.32195000	WM	9	FJ611338	HM014149	/	/	/
IFIU1	Italy (Sardinia)	12.231762	41.792589	WM	9	FJ611338	HM014149	26	JF304856	JF304870
IFIU9	Italy (Sardinia)	12.231762	41.792589	/	12	FJ611337	HM014149	/	/	/
IGEN1	Italy (Sardinia)	11.154399	42.372302	WM	9	FJ611338	HM014149	32	JF304837	HM106408

IGEN9	Italy (Sardinia)	11.154399	42.372302	/	9	FJ611338	HM014149	/	/	/
ILOI3	Italy (Sardinia)	9.49695100	40.84990400	/	9	FJ611338	HM014149	26	JF304841	HM106410
ILOI7	Italy (Sardinia)	9.49695100	40.84990400	WM	9	FJ611338	HM014149	/	/	/
IOSU1	Italy (Sardinia)	9.66244	39.99546	WM	8	FJ611338	HM014153	31	GU984340	HM106410
IOSU9	Italy (Sardinia)	9.66244	39.99546	/	8	FJ611338	HM014153	/	/	/
IPOR1	Italy (Sardinia)	8.414084	39.449174	WM	8	FJ611338	HM014153	33	GU984340	HM106411
IPOR5	Italy (Sardinia)	8.414084	39.449174	/	8	FJ611338	HM014153	/	/	/
ISAN1	Italy (Sardinia)	8.791598	39.098521	WM	9	FJ611338	HM014149	31	GU984340	JF304896
ISAN9	Italy (Sardinia)	8.791598	39.098521	/	9	FJ611338	HM014149	/	/	/
ITEU1	Italy (Sardinia)	8.75824	38.975794	WM	9	FJ611338	HM014149	31	GU984340	HM106410
ITEU9	Italy (Sardinia)	8.75824	38.975794	/	8	FJ611338	HM014153	/	/	/
ICEF1	Italy (Sicily)	13.99276700	38.02900600	/	12	FJ611337	HM014149	31	GU984340	HM106410
ICEF5	Italy (Sicily)	13.99276700	38.02900600	CM	12	FJ611337	HM014149	/	/	/
IPAL1	Italy (Sicily)	13.14523300	38.02748300	/	4	FJ611337	HM014154	16	GU984346	HM106407
IPAL5	Italy (Sicily)	13.14523300	38.02748300	CM	4	FJ611337	HM014154	/	/	/
ISYR1	Italy (Sicily)	14.89486500	37.18398200	/	3	FJ611338	HM014154	16	JF304817	HM106407
ISYR9	Italy (Sicily)	14.89486500	37.18398200	CM	4	FJ611337	HM014154	/	/	/
JKAR1	Jordan	35.617803	31.266779	/	12	FJ611337	HM014149	22	GU984344	HM106405
JKAR5	Jordan	35.617803	31.266779	EM	12	FJ611337	HM014149		/	/
LDMI1	Lebanon	35.497611	33.686722	/	2	FJ611337	HM14157	1	JF304861	JF304880
LDMI9	Lebanon	35.497611	33.686722	CM	1	FJ611337	HM014156	/	/	/
LMAR1	Lebanon	35.568139	33.862972	EM	2	FJ611337	HM14157	36	JF304827	JF304874
LMAR9	Lebanon	35.568139	33.862972	/	2	FJ611337	HM14157	/	/	/
MALT0	Malta	14.394169	35.916833	/	4	FJ611337	HM014154	20	JF304848	JF304884
MRIA1	Morocco	-5.72654300	34.80016500	/	9	FJ611338	HM014149	31	GU984340	HM106410
MRIA5	Morocco	-5.72654300	34.80016500	WM	14	FJ611338	HM014150	/	/	/

MRIB1	Morocco	-5.69763000	34.79624500	/	14	FJ611338	HM014150	26	GU984342	HM106410
MRIB5	Morocco	-5.69763000	34.79624500	WM	14	FJ611338	HM014150	/	/	/
PALE1	Portugal	-7.65744	37.653408	WM	14	FJ611338	HM014150	31	GU984340	HM106410
PALE9	Portugal	-7.65744	37.653408	/	14	FJ611338	HM014150	/	/	/
ASMA1	Portugal (Azores)	-25.161912	36.967147	Mac	6	FJ611338	HM014147	38	JF304834	HM106419
ASMA9	Portugal (Azores)	-25.161912	36.967147	/	7	FJ611338	HM014146	/	/	/
ASMP1	Portugal (Azores)	-25.105245	36.953679	Mac	7	FJ611338	HM014146	39	GU984370	HM106421
ASMP9	Portugal (Azores)	-25.105245	36.953679	/	9	FJ611338	HM014149	/	/	/
MABO1	Portugal (Madeira)	-16.771892	32.752919	Mac	13	FJ611338	HM014153	40	GU984370	HM106417
MABO5	Portugal (Madeira)	-16.771892	32.752919	/	13	FJ611338	HM014153	/	/	/
MAFA1	Portugal (Madeira)	-16.851667	32.78445	Mac	/	/	/	/	/	/
MAV10	Portugal (Madeira)	-17.023961	32.731635	Mac	13	FJ611338	HM014153	41	JF304831	JF304872
ECAD1	Spain	3.28451100	42.30609200	/	9	FJ611338	HM014149	31	GU984340	HM106410
ECAD5	Spain	3.28451100	42.30609200	WM	9	FJ611338	HM014149	/	/	/
ECRE1	Spain	3.29008333	42.31738889	/	9	FJ611338	HM014149	26	JF304841	HM106410
ECRE5	Spain	3.29008333	42.31738889	/	9	FJ611338	HM014149	/	/	/
EDEV1	Spain	-0.31230556	39.34511111	/	8	FJ611338	HM014153	16	JF304853	JF304884
EDEV5	Spain	-0.31230556	39.34511111	CM	4	FJ611337	HM014154	/	/	/
EGUA10	Spain	-6.68666700	37.07972200	/	14	FJ611338	HM014150	/	/	/
EGUA5	Spain	-6.68666700	37.07972200	WM	14	FJ611338	HM014150	31	GU984340	HM106410
EMUR1	Spain	-0.35805556	39.12916667	/	8	FJ611338	HM014153	26	GU984342	HM106410
EMUR5	Spain	-0.35805556	39.12916667	CM	8	FJ611338	HM014153	/	/	/
EROS1	Spain	3.20763889	42.24469444	/	9	FJ611338	HM014149	30	JF304838	HM106410
EROS5	Spain	3.20763889	42.24469444	CM	4	FJ611337	HM014154	/	/	/
ESAL1	Spain	-0.32838889	39.38594444	/	4	FJ611337	HM014154	7	JF304819	JF304890
ESAL5	Spain	-0.32838889	39.38594444	CM	14	FJ611338	HM014150	/	/	/
ETOU1	Spain	-0.66052778	39.16016667	/	8	FJ611338	HM014153	20	JF304844	JF304884
ETOU5	Spain	-0.66052778	39.16016667	CM	8	FJ611338	HM014153	/	/	/
EESP1	Spain (Majorca)	3.37327831	39.70425638	/	8	FJ611338	HM014153	10	GU984353	JF304886

EESP9	Spain (Majorca)	3.37327831	39.70425638	/	4	FJ611337	HM014154	/	/	/
ERAC1	Spain (Majorca)	2.56862274	39.66801409	/	8	FJ611338	HM014153	31	GU984340	HM106410
ERAC9	Spain (Majorca)	2.56862274	39.66801409	WM	8	FJ611338	HM014153	/	/	/
EALG1	Spain (Menorca)	3.93701406	40.04956480	/	8	FJ611338	HM014153	31	GU984340	HM106410
EALG9	Spain (Menorca)	3.93701406	40.04956480	WM	8	FJ611338	HM014153	/	/	/
EMES1	Spain (Menorca)	4.28374941	39.91190183	/	9	FJ611338	HM014149	26	GU984342	HM106410
EMES9	Spain (Menorca)	4.28374941	39.91190183	WM	9	FJ611338	HM014149	/	/	/
EMIT1	Spain (Menorca)	3.97092814	39.93779193	/	9	FJ611338	HM014149	31	GU984340	HM106410
EMIT9	Spain (Menorca)	3.97092814	39.93779193	WM	9	FJ611338	HM014149	/	/	/
SALA1	Syria	35.895833	35.813333	/	1	FJ611337	HM014156	1	GU984349	HM106405
SALA9	Syria	35.895833	35.813333	EM	1	FJ611337	HM014156	/	/	/
SALB1	Syria	35.99556	35.913889	/	1	FJ611337	HM014156	2	GU984350	HM106405
SALB9	Syria	35.99556	35.913889	/	1	FJ611337	HM014156	/	/	/
SALC1	Syria	35.89556	35.813889	/	1	FJ611337	HM014156	11	JF304820	JF304894
SALC9	Syria	35.89556	35.813889	EM	1	FJ611337	HM014156	/	/	/
SBRM1	Syria	36.36000000	34.99444400	/	4	FJ611337	HM014154	1	JF304862	JF304881
SBRM5	Syria	36.36000000	34.99444400	CM	4	FJ611337	HM014154	/	/	/
SKAA1	Syria	36.05313900	34.98622200	/	1	FJ611337	HM014156	2	GU984350	JF304882
SKAA5	Syria	36.05313900	34.98622200	CM	4	FJ611337	HM014154	/	/	/
SKAB1	Syria	36.15313900	35.08622200	/	1	FJ611337	HM014156	2	GU984350	HM106405
SKAB9	Syria	36.15313900	35.08622200	EM	1	FJ611337	HM014156	/	/	/
TFAH1	Tunisia	10.12916700	36.38583300	/	4	FJ611337	HM014154	31	GU984340	HM106410
TFAH5	Tunisia	10.12916700	36.38583300	CM	4	FJ611337	HM014154	/	/	/
TGAL1	Tunisia	8.938711	37.52724	/	9	FJ611338	HM014149	29	GU984342	HM106410
TGAL9	Tunisia	8.938711	37.52724	WM	9	FJ611338	HM014149	/	/	/
TKRO1	Tunisia	8.67625	36.691667	WM	/	/	/	/	/	/
TZAG1	Tunisia	10.12916667	36.38583333	/	4	FJ611337	HM014154	/	/	/
TZAG5	Tunisia	10.12916667	36.38583333	CM	4	FJ611337	HM014154	34	JF304866	JF304898
TZEM1	Tunisia	10.81144444	37.12844444	/	12	FJ611337	HM014149	28	JF304825	JF304886

TZEM3	Tunisia	10.81144444	37.12844444	WM	9	FJ611338	HM014149	/	/
TUAC1	Turkey	27.349717	37.746183	/	4	FJ611337	HM014154	16	JF304857 JF304884
TUAC2	Turkey	27.349717	37.746183	/	4	FJ611337	HM014154	/	/ /
TUAG1	Turkey	29.690783	36.218967	/	2	FJ611337	HM14157	2	GU984350 HM106405
TUAG2	Turkey	29.690783	36.218967	/	2	FJ611337	HM14157	/	/ /
TUAR1	Turkey	30.09125	36.484433	/	10	FJ611337	HM014154	20	JF304850 JF304889
TUAR2	Turkey	30.09125	36.484433	/	4	FJ611337	HM014154	/	/ /
TUBR1	Turkey	29.947633	36.249167	/	2	FJ611337	HM14157	14	GU984358 JF304885
TUBR2	Turkey	29.947633	36.249167	CM	2	FJ611337	HM14157	/	/ /
TUCE1	Turkey	27.176267	37.6998	/	4	FJ611337	HM014154	20	JF304851 JF304891
TUCE2	Turkey	27.176267	37.6998	CM	4	FJ611337	HM014154	/	/ /
TUDA1	Turkey	27.85855	36.767567	/	2	FJ611337	HM14157	2	JF304854 JF304878
TUDA2	Turkey	27.85855	36.767567	CM	2	FJ611337	HM14157	/	/ /
TUDE1	Turkey	29.943783	36.229083	/	2	FJ611337	HM14157	18	JF304816 JF304885
TUDE2	Turkey	29.943783	36.229083	/	2	FJ611337	HM14157	/	/ /
TUDL1	Turkey	28.668417	36.836367	/	2	FJ611337	HM14157	37	JF304823 JF304875
TUDL2	Turkey	28.668417	36.836367	/	2	FJ611337	HM14157	/	/ /
TUFE1	Turkey	29.112733	36.475867	/	4	FJ611337	HM014154	20	JF304844 JF304884
TUFE2	Turkey	29.112733	36.475867	/	4	FJ611337	HM014154	/	/ /
TUGO1	Turkey	28.963717	36.746333	/	2	FJ611337	HM14157	2	GU984350 HM106405
TUGO2	Turkey	28.963717	36.746333	CM	2	FJ611337	HM14157	/	/ /
TUKA1	Turkey	27.56005	37.434117	/	4	FJ611337	HM014154	15	JF304856 HM106406
TUKA2	Turkey	27.56005	37.434117	/	4	FJ611337	HM014154	/	/ /
TUKR1	Turkey	27.89656700	37.30085000	/	2	FJ611337	HM14157	2	GU984350 HM106405
TUKR2	Turkey	27.89656700	37.30085000	CM	4	FJ611337	HM014154	/	/ /
TUMA1	Turkey	29.295883	36.9858	/	2	FJ611337	HM14157	3	GU984351 JF304877
TUMA2	Turkey	29.295883	36.9858	/	2	FJ611337	HM14157	/	/ /
TUME1	Turkey	27.577917	36.70145	/	4	FJ611337	HM014154	11	GU984353 JF304892
TUME2	Turkey	27.577917	36.70145	/	4	FJ611337	HM014154	/	/ /
TUSA1	Turkey	33.298983	42.007267	CM	/	/	/	/	/ /
TUSB1	Turkey	34.176556	41.940595	CM	/	/	/	/	/ /
TUSI1	Turkey	34.950833	42.087594	CM	4	FJ611337	HM014154	8	JF304846 JF304893
TUSI3	Turkey	35.050833	42.187594	/	4	FJ611337	HM014154	8	JF304835 JF304893

TUSI5	Turkey	35.150833	42.287594	/	4	FJ611337	HM014154	1	JF304863	JF304883
TUSI7	Turkey	35.250833	42.387594	/	4	FJ611337	HM014154	10	JF304829	JF304873
TUSI9	Turkey	35.350833	42.487594	/	4	FJ611337	HM014154	10	JF304830	JF304873
TUTE1	Turkey	28.69545	36.866983	/	2	FJ611337	HM14157	6	JF304824	JF304900
TUTE2	Turkey	28.69545	36.866983	/	2	FJ611337	HM14157	/	/	/











Table S2. AIC scores and number of parameters for fitted MAXENT models.

Akaike Information Criterion (AIC) scores and number of parameters for all fitted MAXENT models using all possible simple and combination of features except "threshold": L = linear, Q = quadratic, P = product.

Features combination	Number of parameters	Delta AIC	AIC score
L Q	12	0	85779.3
Q	6	10139.8	95919.1
L	6	10931.8	96711.1
L Q P	26	20735.3	106514.6
L P	21	29335.3	115114.6
Q P	21	30176.3	115955.6

Table S3. Bibliographic review of the main imprints left by past environmental changes on Mediterranean widespread, Tertiary-originated, and/or thermophilous woody species, combining genetic, distribution modelling and palaeoecological data.

Bibliographic review of the main imprints left by past environmental changes on Mediterranean widespread, Tertiary-originated, and/or thermophilous woody species, combining genetic, distribution modelling and palaeoecological data. Mean values of cold resistance for vegetative organs in adult specimens are those causing 50% damage to leaf buds and cambium (based on Larcher, 1981, 2000; Quézel & Médail, 2003; Flexas *et al.*, 2014).

Taxa	Data available	Phylogeographical patterns	1. Main inferences from phylogeography	2. Main predictions from SDM	Cold resistance	References
<i>Arbutus unedo</i> L. (Ericaceae)	 - 4 pDNA (2,401-2,449 bp: <i>trnH</i> (GUG)- <i>psbA</i> , <i>trnL</i> (UAG)- <i>rpl32</i> , <i>trnT</i> (UGU)- <i>trnL</i> (UAA) and Intron L; <i>n</i> = 207, 23 pops) > 28 haplotypes  - Molecular dating  - (Map of LGM climatic conditions)	 2 main genetic clusters	<ul style="list-style-type: none"> - Tertiary divergence between <i>A. unedo</i> (WM) / <i>A. andrachne</i> (EM) - Western diversification of <i>A. unedo</i> during the last 700 ka (hardest Pleistocene glaciations) and eastward migrations. - Key role of glacial refugia (WM + NAfrica) + Refugia within refugia model. - Recent post-glacial migration to Ireland from Iberia. - Partial gene flow barriers Straits of Sicily and Gibraltar 	Not available	<ul style="list-style-type: none"> - Leaf buds: -17°C - Cambium: -18°C 	- Santiso <i>et al.</i> , 2015, 2016
<i>Buxus balearica</i> Lam. (Buxaceae)	 - nrDNA (662 bp: <i>ITS</i> ; <i>n</i> = 15, 15 pops with cloning) > 19 ribotypes  -  -		<ul style="list-style-type: none"> - Poor phylogeographical resolution of nrDNA ITS sequences. EM (Anatolia) retained ancestral ribosomal sequences. 	Not available	<ul style="list-style-type: none"> - Not a cold-tolerant taxon: in unglaciated southern refugia, not beyond 39°N. 	- Rosselló <i>et al.</i> , 2007
<i>Celtis australis</i> L. (Cannabaceae)	 - 3 pDNA (3,134 bp: <i>rps16</i> , <i>rpl32</i> - <i>trnL</i> , <i>trnQ</i> -5'- <i>rps16</i> ; <i>n</i> = 328, 39 pops)  - 20 pDNA SSRs (<i>n</i> = 328, 39 pops)	 No pDNA variability	<ul style="list-style-type: none"> - Recent recolonization after drastic contraction or even disappearance in the Mediterranean is supposed. - A high sensitivity of riparian corridors to frost during the LGM is suggested. 	Not available		- Mateu-Andrés <i>et al.</i> , 2015



***Chamaerops humilis* L.**

(Palmae)



- 3 AFLP ($n = 220$, 22 pops)
- Molecular dating (not based on sequence divergence)
- PMIP2 Worldclim Maxent: LIG, LGM, Present
- Eocene fossils



4 main genetic clusters
(but weakly sampled)

- Strong divergence in the WM, potentially related to a Miocene W/E vicariance (5.83-8.32 Ma).

- Evidence for Pleistocene expansion and admixture.

- Range contraction stronger for LIG than LGM, mainly for the continental areas of France-Italy and E Spain-Sardinia-NE Morocco.

- Very low likelihood of occurrence for Corsica contrary to other islands.

- Leaf buds: -11.5°C

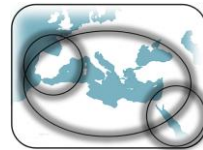
- García-Castaño *et al.*, 2014

***Erica arborea* L.**

(Ericaceae)



- 3 pDNA (1,876 bp: *atpB-rbcL*, *MatK*, *trnH-psbA* and *rp16*; $n = 105$) > 19 haplotypes
- Molecular dating
- PMIP2 Worldclim Maxent (GPS $n = 135$): LGM, Present (Macaronesia and WM only: *Erica scoparia*)
- Fossils ($n = 4$)



3 main genetic clusters

- Pliocene divergence of 3 genetic clusters (5.82-1.49 Ma) with a E/W bipolarisation of genetic diversity.

- Two waves of expansions in the Miocene and Pleistocene.

- One widespread haplotype supports recent events of long distance dispersal.

- Migrations to Macaronesia and Sahara (Tibesti Mt).

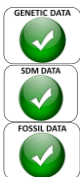
- Range contraction during the LGM.

- No suitable area predicted for LGM in W Europe but refugia along the African Atlantic coast.

- Désamoré *et al.*, 2011, 2012

***Laurus nobilis* L.**

(Lauraceae)



- 2 pDNA (2,562 bp: *trnK-MatK* and *trnD-T*; $n = 57$) > 6 haplotypes
- 2 AFLP ($n = 62$, 11 pops)
- Haywood & Valdes 2004 simulations and PMIP models, MaxEnt (GPS $n = 925$): Middle Pliocene (3 Ma), LGM, Present, Future
- Pliocene fossils ($n = 36$)



3 main genetic clusters

- Longitudinal geographical structure related to isolation of WM and EM genetic clusters with strong barriers in the East (Floristic Rechinger's line).

- The WM genetic cluster is more diverse and expanded eastward.

- One widespread haplotype supports recent events of long distance dispersal.

- Large suitable areas during the Pliocene (niche conservatism) and strong LGM contraction.

- Partial recolonisation during suitable interglacial periods.

- Leaf buds: -10°C

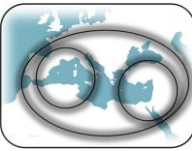

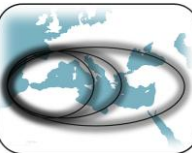
- Cambium: -14°C
















- Arroyo-García *et al.*, 2001













- Rodríguez-Sánchez & Arroyo, 2008

- Rodríguez-Sánchez *et al.*, 2009

- Migrations to Macaronesia (*Laurus azorica*).

<p><i>Myrtus communis</i> L. (Myrtaceae)</p>	<ul style="list-style-type: none"> - 2 pDNA (932 bp: <i>trnL-trnF</i> and <i>rp12-trnH</i>; <i>n</i> = 309) > 12 haplotypes - 2 nrDNA (1,011 bp: <i>ITS</i> and <i>ETS</i>; <i>n</i> = 176) >39 ribotypes - 2 AFLP (<i>n</i> = 118) - Molecular dating - CMIP5 Worldclim, MaxEnt (GPS <i>n</i> = 4,168): LIG, LGM, Mid-Holocene, Present - Pleistocene pollen (<i>n</i> = 76) - Neogene fossils 	 <p>3 main genetic clusters</p>	<ul style="list-style-type: none"> - A vicariance event in the late Miocene led to W/E bipolarisation of genetic diversity. - Higher diversification in WM with eastward migration. CM genetic cluster with potentially a central origin, migrated westward and eastward (one widespread haplotype). EM genetic cluster remained geographically restricted. - Migrations to Macaronesia and Sahara (<i>Myrtus nivellei</i>). 	<ul style="list-style-type: none"> - Range contraction predicted for LGM. - Comparison of suitability maps among three periods reported a lack of long-term refugia, supporting range shift as the main response to climate oscillation. 	<ul style="list-style-type: none"> - Leaf buds: -11°C - Cambium: -17°C 	<ul style="list-style-type: none"> - Migliore <i>et al.</i>, 2012, 2013 - This study
<p><i>Nerium oleander</i> L. (Apocynaceae)</p>	<ul style="list-style-type: none"> - 3 pDNA (3,134 bp: <i>rps16</i>, <i>rp132-trnL</i>, <i>trnQ-5'-rps16</i>; <i>n</i> = 448, 53 pops) > 3 haplotypes (2 Sahara +1 Med.) - 20 pDNA SSRs (<i>n</i> = 448, 53 pops) - Molecular dating 	 <p>No pDNA variability</p>	<ul style="list-style-type: none"> - Drastic bottleneck supposed to explain the absence of pDNA variability. - Unique divergence detected Sahara/ Med: 7.2-1.2 Ma: migrations from the Saharan refugia? - High sensitivity of riparian corridors to frost during the LGM supposed. 	<p>Not available</p>	<ul style="list-style-type: none"> - Leaf buds: -12°C - Cambium: -14°C 	<ul style="list-style-type: none"> - Mateu-Andrés <i>et al.</i>, 2015
<p><i>Olea europaea</i> L. (Oleaceae)</p>	<ul style="list-style-type: none"> - pDNA genome profiling (61 loci; <i>n</i> = 1,263 oleasters) > 48 haplotypes - Molecular dating - PMIP2 Worldclim, MaxEnt (GPS <i>n</i> = 88): LIG, LGM, Present - LGM pollen/fossils (<i>n</i> = 14/9) 	 <p>3 main genetic clusters</p>	<ul style="list-style-type: none"> - Divergence between Oleaster lineages started during the late Pliocene. - Despite long distance dispersal and admixture with cultivated Olives, a strong W/E differentiation is still present. Several haplotypes restricted to the East. One genetic cluster could have central origin. - Migrations/introgression in Macaronesia/Sahara. 	<ul style="list-style-type: none"> - Range contraction predicted during the LGM, with 3 main long-term refugia: Strait of Gibraltar, Aegean area, Near East (including Cyprus). 	<ul style="list-style-type: none"> - Leaf buds: -13°C - Cambium: -20°C 	<ul style="list-style-type: none"> - Besnard <i>et al.</i>, 2007, 2009, 2013 - Díez <i>et al.</i>, 2015 - Besnard & Rubio de Casas, 2016 - Díez & Gaut., 2016

<p><i>Pinus halepensis</i> Mill.</p> <p>(Pinaceae)</p>	<p> GENETIC DATA</p> <p> SDM DATA - 9 cpSSRs (10 pops, 9-16 seeds /stand)</p> <p> FOSSIL DATA</p>		<p>- Low phylogeographical resolution: a westward expansion from a unique refugium in Southern Balkans.</p> <p>- Strong foundation events could explain the lower genetic diversity in WM populations.</p>	<p><i>Not available</i></p>	<p>- Cambium: -22°C</p>	<p>- Bucci <i>et al.</i>, 1998</p> <p>- Grivet <i>et al.</i>, 2009</p>
<p><i>Pinus pinaster</i> Alton</p> <p>(Pinaceae)</p>	<p> GENETIC DATA - 7 pDNA sequences + RFLP > 15 haplotypes</p> <p> SDM DATA - 4 mtDNA RFLP (<i>n</i> = 570, 57 pops) > 3 mitotypes</p> <p> FOSSIL DATA - 5 cpSSRs (<i>n</i> = 1339, 48 pops) and genetic interpolation</p> <p>- Worldclim, GLMs /GAMs /RF /CTA /MaxEnt (GPS <i>n</i> = 128,653): Present</p>	 <p>3 main genetic clusters</p>	<p>- Eight gene pools organized in three main genetic clusters.</p> <p>- Post glacial expansions from a minimum of 3 refugia to explain the observed phylogeography and pattern of population genetic diversity.</p>	<p>- Different climatic niches among the 3 genetic clusters.</p>		<p>- Burban & Petit, 2003</p> <p>- Bucci <i>et al.</i>, 2007</p> <p>- Serra-Varela <i>et al.</i>, 2015</p>
<p><i>Pinus pinea</i> L.</p> <p>(Pinaceae)</p>	<p> GENETIC DATA</p> <p> SDM DATA - 37 isozymes (<i>n</i> = 573, 17 pops)</p> <p> FOSSIL DATA - 12 pDNA SSR (<i>n</i> = 856, 34 pops)</p>	 <p>No pDNA variability</p>	<p>- Demographic bottleneck suggested: 1 WM haplotype and 2 in the EM.</p> <p>- After the bottleneck long distance dispersal or human-mediated dispersal could explain the current Mediterranean range.</p>	<p><i>Not available</i></p>	<p>- Leaf buds: -16°C</p> <p>- Cambium: -19°C</p>	<p>- Fallour <i>et al.</i>, 1997</p> <p>- Vendramin <i>et al.</i>, 2008</p>
<p><i>Quercus cerris</i> L.</p> <p>(Fagaceae)</p>	<p> GENETIC DATA - 6 pDNA SSR (<i>n</i> = 1,175, 192 pops) > 35 haplotypes</p> <p> SDM DATA - Molecular dating</p> <p> FOSSIL DATA - Demographic history DIYABC</p> <p>- Pollen and fossil review in palaeoecological records for estimating persistence</p>	 <p>3 main genetic clusters</p>	<p>- Genetic clusters organized longitudinally, with an eastern one, centred on Anotalia, inferred as ancestral.</p> <p>- The split between the Eastern (Anotalia) and Central (Balkan) genetic clusters occurred before in the Early Pliocene whereas the split between the central and western (Italy) genetic clusters is dated to the Mid Pleistocene.</p>	<p><i>Not available</i></p>		<p>- Bagnoli <i>et al.</i>, 2016</p>

			- Haplotype sharing between <i>Q. suber</i> and <i>Q. cerris</i> in Pleistocene Italian glacial refugia, as hypothesis.			
<i>Quercus coccifera</i> L. / <i>Q. calliprinos</i> Webb (Fagaceae)	 - 5 pDNA PCR-RFLP ($n = 420$, 50 pops)  - 1 nrDNA (594 bp: <i>ITS</i> ; $n = 6$) - 5 AFLP ($n = 19$, 19 pops)  - 7 allozymes ($n = 609$, 24 pops)	 2 main genetic clusters	<ul style="list-style-type: none"> - Genetic clusters are corresponding to <i>Q. calliprinos</i> in EM / <i>Q. coccifera</i> in WM. - EM genetic cluster: higher genetic diversity and stronger genetic structure. - Bottleneck during the LGM followed by rapid post-glacial recolonisations suggested to explain the lower diversity and differentiation in the WM. 	Not available	<ul style="list-style-type: none"> - Leaf buds: -13°C - Cambium: -21°C 	<ul style="list-style-type: none"> - Lopez de Heredia <i>et al.</i>, 2007 - Toumi & Lumaret, 2010
<i>Quercus ilex</i> L. (Fagaceae)	 - 5 pDNA PCR-RFLP ($n = 1,116$, 121 pops)  - pDNA PCR RFLP ($n \approx 697$, 174 pops) - 1 nrDNA (592 bp: <i>ITS</i> ; $n = 11$)  - 5 AFLP ($n = 41$, 39 pops)	 2 main genetic clusters	<ul style="list-style-type: none"> - Strong imprint of glaciations with two main genetic clusters corresponding to the main peninsula refugia. - Admixture and post-glacial contact zone of lineages in the Rhône Valley (France). Extensive hybridization with <i>Q. coccifera</i> and <i>Q. suber</i>. 	Not available	<ul style="list-style-type: none"> - Leaf buds: -17°C - Cambium: -28°C 	<ul style="list-style-type: none"> - Lumaret <i>et al.</i>, 2002 - Lopez de Heredia <i>et al.</i>, 2007
<i>Quercus suber</i> L. (Fagaceae)	 - 14 pDNA SSRs ($n = 508$, 110 pops) > 5 haplotypes - 7/5 pDNA PCR RFLP ($n \approx 365$, 91 pops/ $n = 854$, 94 pops)  - 1 nrDNA (617 bp: <i>ITS</i> ; $n = 17$) - 5 AFLP ($n = 34$, 32 pops)  - PMIP3 Worldclim, openModeller algorithms (GPS $n = 63,733$): LIG, LGM, Mid-Holocene, Present - Pleistocene pollen and tree fossils ($n = 17$)	 3 main genetic clusters	<ul style="list-style-type: none"> - 3 genetic clusters (W. Iberia, Morocco / Algeria, Tunisia, Tyrrhenian islands / Italy, Sicily) considered under a hypothesis of deep divergence that could be related to Oligocene-Miocene palaeogeography, but a molecular dating approaches is lacking to test it. 	<ul style="list-style-type: none"> - Long-term persistence in Mediterranean without striking range contraction or shift, even during the LGM. 	<ul style="list-style-type: none"> - Leaf buds: -16°C - Cambium: -26°C 	<ul style="list-style-type: none"> - Lumaret <i>et al.</i>, 2005 - Lopez de Heredia <i>et al.</i>, 2007 - Magri <i>et al.</i>, 2007 - Vessella <i>et al.</i>, 2015

References:

- Arroyo-García R, Martínez-Zapater JM, Fernández-Prieto JA, Álvarez-Arbesu R. 2001. AFLP evaluation of genetic similarity among laurel populations (*Laurus* L.). *Euphytica* **122**: 155-164.
- Bagnoli F, Tsuda Y, Fineschi S, Bruschi P, Magri D, Zhelev P, Paule L, Simeone MC, González-Martínez SC, Vendramin GG. 2016. Combining molecular and fossil data to infer demographic history of *Quercus cerris*: insights on European eastern glacial refugia. *Journal of Biogeography* **43**: 679-690.
- Besnard G, Rubio de Casas R. 2016. Single vs multiple independent olive domestications: the jury is (still) out. *New Phytologist* **209**: 466-470.
- Besnard G, Rubio de Casas R, Christin P-A, Vargas P. 2009. Phylogenetics of *Olea* (Oleaceae) based on plastid and nuclear ribosomal DNA sequences: Tertiary climatic shifts and lineage differentiation times. *Annals of Botany* **104**: 143-160.
- Besnard G, Henry P, Wille L, Cooke D, Chapuis E. 2007. On the origin of the invasive olives (*Olea europaea* L., Oleaceae). *Heredity* **99**: 608-619.
- Besnard G, Khadari B, Navascués M, Fernández-Mazuecos M, Bakkali AE, Arrigo N, Baali-Cherif D, Brunini-Bronzini de Caraffa V, Santoni S, Vargas P, Savolainen V. 2013. The complex history of the olive tree: from Late Quaternary diversification of Mediterranean lineages to primary domestication in the northern Levant. *Proceedings of the Royal Society B: Biological Sciences* **280**: 20122833.
- Boratynski A, Lewandowski A, Boratynska K, Montserrat JM, Romo A. 2009. High level of genetic differentiation of *Juniperus phoenicea* (Cupressaceae) in the Mediterranean region: geographic implications. *Plant Systematics and Evolution* **277**: 163-172.
- Bucci G, Anzidei M, Madaghiele A, Vendramin GG. 1998. Detection of haplotypic variation and natural hybridization in *halepensis*-complex pine species using chloroplast simple sequence repeat (SSR) markers. *Molecular Ecology* **7**: 1633-1643.
- Bucci G, Gonzalez-Martinez SC, Le Provost G, Plomion C, Ribeiro MM, Sebastiani F, Alia R, Vendramin GG. 2007. Range-wide phylogeography and gene zones in *Pinus pinaster* Ait. revealed by chloroplast microsatellite markers. *Molecular Ecology* **16**: 2137-2153.
- Burban C, Petit RJ. 2003. Phylogeography of maritime pine inferred with organelle markers having contrasted inheritance. *Molecular Ecology* **12**: 1487-1495.
- Désamóré A, Laenen B, Devos N, Popp M, Gonzalez-Mancebo JM, Carine MA, Vanderpoorten A. 2011. Out of Africa: north-westwards Pleistocene expansions of the heather *Erica arborea*. *Journal of Biogeography* **38**: 164-176.
- Désamóré A, Laenen B, Gonzalez-Mancebo JM, Jaen Molina R, Bystrakova N, Martinez-Klimova E, Carine MA, Vanderpoorten A. 2012. Inverted patterns of genetic diversity in continental and island populations of the heather *Erica scoparia* s.l. *Journal of Biogeography* **39**: 574-584.
- Díez CM, Gaut BS. 2016. The jury may be out, but it is important that it deliberates: a response to Besnard and Rubio de Casas about olive domestication. *New Phytologist* **209**: 471-473.
- Díez CM, Trujillo I, Martínez-Urdiroz N, Barranco D, Rallo L, Marfil P, Gaut BS. 2015. Olive domestication and diversification in the Mediterranean Basin. *New Phytologist* **206**: 436-447.
- Fallour D, Fady B, Lefèvre F. 1997. Study on isozyme variation in *Pinus pinea* L.: evidence for low polymorphism. *Silvae Genetica* **46**: 201-207.
- Flexas J, Diaz-Espejo A, Gago J, Gallé A, Galmés J, Gulías J, Medrano H. 2014. Photosynthetic limitations in Mediterranean plants: a review. *Environmental and Experimental Botany* **103**: 12-23.
- García-Castaño JL, Terrab A, Ortiz MÁ, Stuessy TF, Talavera S. 2014. Patterns of phylogeography and vicariance of *Chamaerops humilis* L. (Palmae). *Turkish Journal of Botany* **38**: 1132-1146.
- Grivet D, Sebastiani F, González-Martínez SC, Vendramin GG. 2009. Patterns of polymorphism resulting from long-range colonization in the Mediterranean conifer Aleppo pine. *New Phytologist* **184**: 1016-1028.
- Larcher W. 1981. Low temperature effects on Mediterranean sclerophylls: an unconventional viewpoint. In: Margaris NS, Mooney HA, eds. *Tasks for Vegetation Science. Components of productivity of Mediterranean-climate regions Basic and applied aspects*. Netherlands: Springer, 259-266.
- Larcher W. 2000. Temperature stress and survival ability of Mediterranean sclerophyllous plants. *Plant Biosystems* **134**: 279-295.
- Lopez de Heredia U, Jimenez P, Collada C, Simeone MC, Bellarosa R, Schirone B, Cervera MT, Gil L. 2007. Multi-marker phylogeny of three evergreen oaks reveals vicariant patterns in the Western Mediterranean. *Taxon* **56**: 1209-1220.
- Lumaret R, Mir C, Michaud H, Raynal V. 2002. Phylogeographical variation of chloroplast DNA in holm oak (*Quercus ilex* L.). *Molecular Ecology* **11**: 2327-2336.
- Lumaret R, Tryphon-Dionnet M, Michaud H, Sanuy A, Ipotesi E, Born C, Mir C. 2005. Phylogeographical variation of chloroplast DNA in Cork Oak (*Quercus suber*). *Annals of Botany* **96**: 853-861.
- Magri D, Fineschi S, Bellarosa R, Buonamici A, Sebastiani F, Schirone B, Simeone MC, Vendramin GG. 2007. The distribution of *Quercus suber* chloroplast haplotypes matches the palaeogeographical history of the western Mediterranean. *Molecular Ecology* **16**: 5259-5266.
- Mateu-Andrés I, Czurana M-J, Aguilera A, Boisset F, Guara M, Laguna E, Currás R, Ferrer P, Vela E, Puche MF, Pedrola-Monfort J. 2015. Plastid DNA Homogeneity in *Celtis australis* L. (Cannabaceae) and *Nerium oleander* L. (Apocynaceae) throughout the Mediterranean Basin. *International Journal of Plant Sciences* **176**: 421-432.
- Migliore J, Baumel A, Juin M, Médail F. 2012. From Mediterranean shores to central Saharan mountains: key phylogeographical insights from the genus *Myrtus*. *Journal of Biogeography* **39**: 942-956.
- Rodríguez-Sánchez F, Arroyo J. 2008. Reconstructing the demise of Tethyan plants: climate-driven range dynamics of *Laurus* since the Pliocene. *Global Ecology and Biogeography* **17**: 685-695.
- Rodríguez-Sánchez F, Guzman B, Valido A, Vargas P, Arroyo J. 2009. Late Neogene history of the laurel tree (*Laurus* L., Lauraceae) based on phylogeographical analyses of Mediterranean and Macaronesian populations. *Journal of Biogeography* **36**: 1270-1281.

- Rossello JA, Lazaro A, Cosin R, Molins A. 2007.** A phylogeographic split in *Buxus balearica* (Buxaceae) as evidenced by nuclear ribosomal markers: when ITS paralogues are welcome. *Journal of Molecular Evolution* **64**: 143-157.
- Santiso X, Lopez L, Retuerto R, Barreiro R. 2016.** Phylogeography of a widespread species: Pre-glacial vicariance, refugia, occasional blocking straits and long-distance migrations. *AoB Plants*: plw003.
- Santiso X, López L, Gilbert KJ, Barreiro R, Whitlock MC, Retuerto R. 2015.** Patterns of genetic variation within and among populations in *Arbutus unedo* and its relation with selection and evolvability. *Perspectives in Plant Ecology, Evolution and Systematics* **17**: 185-192.
- Serra-Varela MJ, Grivet D, Vincenot L, Broennimann O, Gonzalo-Jiménez J, Zimmermann NE. 2015.** Does phylogeographical structure relate to climatic niche divergence? A test using maritime pine (*Pinus pinaster* Ait.). *Global Ecology and Biogeography* **24**: 1302-1313.
- Toumi L, Lumaret R. 2010.** Genetic variation and evolutionary history of holly oak: a circum-Mediterranean species-complex [*Quercus coccifera* L./*Q. calliprinos* (Webb) Holmboe, Fagaceae]. *Plant Systematics and Evolution* **290**: 159-171.
- Vendramin GG, Fady B, González-Martínez SC, Hu FS, Scotti I, Sebastiani F, Soto A, Petit RJ. 2008.** Genetically depauperate but widespread: the case of an emblematic Mediterranean Pine. *Evolution* **62**: 680-688.
- Vessella F, Simeone MC, Schirone B. 2015.** *Quercus suber* range dynamics by ecological niche modelling: from the Last Interglacial to present time. *Quaternary Science Reviews* **119**: 85-93.